PHYSICS *and* ASTRONOMY *of the* MOON

Edited by
ZDENĚK KOPAL
Department of Astronomy
University of Manchester

1962
ACADEMIC PRESS, New York and London

CHAPTER 8

Interpretation of Lunar Craters†

EUGENE M. SHOEMAKER

I. Introduction

The dominant surface features of the Moon are approximately circular depressions, which may be designated by the general term crater. Employed in this way, the word crater is used in its original sense—a cup-shaped topographic feature—after the Greek root κρατερ (cup or bowl)‡. Solution of the origin of the lunarcraters is fundamental to the unravelling of the history of the Moon and may shed much light on the history of the terrestrial planets as well.

Most geological and probably most selenological processes are too

† Publication authorized by the Director, U.S. Geological Survey.

‡ Despite the special niche in an elaborate classification assigned to the term crater by selenographers, and whatever connotations of volcanism this word may have had to various authors in the past, the meaning of crater has become much more general in current scientific literature; here it is employed as an inclusive descriptive term without prejudice as to mode of origin.

complex to be safely deduced from first principles. On the other hand, we may reasonably expect the same physical laws to apply on the Moon as on Earth, and we may also expect the rocks of the Moon to share some of the same range of chemical and physical properties as the rocks of the Earth. Undoubtedly there are differences—probably critical differences—in the physical, chemical, and historical setting of the surface of the Earth and Moon, and, indeed, there are striking differences in their topography. But if the problem is approached by analogy, attention may be focused on those features which are similar or the same in two different environments; the closer the comparison that can be made, the stronger is the argument.

There is nothing new in the thesis that close comparison of lunar features with possible terrestrial homologues will prove fruitful, for it has been followed in lunar studies since the time of Galileo. The justification for taking it up anew is that our understanding of terrestrial phenomena relevant to the Moon has advanced greatly over the course of the years and particularly in the last two decades. In applying analogical reasoning, moreover, great care must be exercised in scaling. This has been the major single pitfall in past comparisons of the features either of the Earth or of experimental models with those of the Moon. A jump of one order of magnitude in linear dimension and sometimes more has commonly been made in comparing terrestrial craters with lunar craters, and a jump of six orders of magnitude is commonly made in going from model experiments to the Moon.†

In the pages that follow, the characteristics and origin of terrestrial features that resemble lunar craters are first reviewed and criteria are established by which results of various crater-forming processes on the Moon might be distinguished. The history of a selected region is then examined in the light of these criteria.

It would be impossible to take cognizance of all the pertinent geological and astronomical literature in a paper of this scope. I shall draw primarily, therefore, on personal research on the mechanics of maars and of meteorite impact craters and illustrate the discussion, where appropriate, with geological and experimental features with which I have had a direct acquaintance through field work. No attempt is made to explain all the surface features of the Moon. Rather, a few examples are analysed in detail consonant with the present state of the art in lunar telescopic observation and photography and in space exploration.

† A first approximation to many of the scaling relations can be made from elementary considerations of dimensional analysis. A paper by Hubbert (1937) gives an excellent introduction to the scaling or modelling relations of the physical properties of rocks.

II. Crater-forming Processes

In his biography of G. K. Gilbert, the American geomorphologist W. M. Davis wrote (1926, pp. 185–186):

> "It has been remarked that the majority of astronomers explain the craters of the moon by volcanic eruption—that is, by an essentially geological process—while a considerable number of geologists are inclined to explain them by the impact of bodies falling upon the moon—that is, by an essentially astronomical process. This suggests that each group of scientists find the craters so difficult to explain by processes with which they are professionally familiar that they have recourse to a process belonging in another field than their own, with which they are probably imperfectly acquainted, and with which they therefore feel freer to take liberties."

Since the time of Davis' writing, the division of opinion appears to have shifted, and the literature prior to 1900 reveals that a volcanic origin of the craters had been the prevailing consensus of both groups of scientists. It is nevertheless true that the selenological contributions of geologists and the selenological papers written by astronomers, have comprised two somewhat independent bodies of literature, at least after the time of the great naturalists such as von Humboldt and of the astronomer-volcanologist, Julius Schmidt.

Probably both volcanic and impact hypotheses for the origin of the lunar craters are nearly as old as the discovery of the craters by Galileo in 1610. Robert Hooke (1665, p. 243) compared the lunar craters with those formed on the surface of boiling alabaster and with craters formed by dropping bullets on wet clay, but he rejected the impact analogy because "it would be difficult to imagine whence those bodies should come". By the beginning of the 19th century a volcanic origin for the lunar craters appears to have been nearly universally accepted among the scientists of the time. A volcanic origin had been championed by Kant (1785), and the astronomer Herschel (1787) had even reported what he believed to be observations of volcanic eruptions on the Moon. But it should be recalled that the extraterrestrial origin of meteorites was not then generally accepted. After the meteorite shower at L'Aigle in France in 1803, which awakened widespread interest in meteorites, the impact hypothesis for the origin of the lunar craters was revived by Gruithuisen (1829), who also appears to have anticipated the planetesimal accretion hypothesis for the origin of the Moon. Many of Gruithuisen's views were extreme, however, and most of the principal selenologists continued to accept, without apparent hesitation, some form of volcanism as the crater-forming process.

The later history of astronomical thought on the origin of lunar

surface features has been reviewed repeatedly (Nevill, 1876; Goodacre, 1931; Baldwin, 1949; Wilkins and Moore, 1955) and need not be repeated in detail here. It is appropriate, on the other hand, to trace briefly the evolution of thought in papers written from the geological point of view, which are less well known. An excellent earlier review of the geological viewpoint was given by Wegener (1921).

A. Geological Trend of Inquiry

A distinct geological line of thought on lunar craters may be considered to have begun with the rise of the science of volcanology. J. B. A. L. L. Élie de Beaumont explained the lunar craters in terms of von Buch's now rejected theory of "craters of elevation", whereby calderas and certain other types of volcanic craters were considered to have been formed by updoming of horizontally deposited layers of volcanic material around a central depression. He compared a large circular basin on the island of Ceylon with lunar craters (Élie de Beaumont, 1831), and later published (Élie de Beaumont, 1843) an extensive list of crater-form terrestrial features with which lunar craters might be compared. Most of the terrestrial craters on this list were of volcanic origin, but the largest, the Bohemian basin, about 120 miles across is a roughly circular region ringed with mountains of non-volcanic origin. It was originally compared by Galileo with the craters of the Moon.

After an expedition to the Hawaiian Islands, the American geologist Dana (1846) compared the craters of the Moon with the calderas and other features associated with the Hawaiian shield volcanoes. Much later the astronomer W. H. Pickering (1906) repeated this comparison in more detail. The English volcanologist G. P. Scrope (1862, p. 233) appears to have been the first to point out similarities between lunar craters and the maars of the Phlegraean fields, near the Bay of Naples. Again, the suggestion of the geologist was later elaborated by astronomers, in this case by Nasmyth and Carpenter (1885). Von Humboldt (1863, p. 155) reasserted von Buch's theory of "craters of elevation" with reference to the craters of the Moon in his encyclopedic work, "Cosmos", though he recognized a disparity in form and size between the lunar craters and most terrestrial volcanic craters.

A fundamental advance in the study of the origin of the Moon's surface features was made in 1893 by G. K. Gilbert, then Chief Geologist of the United States Geological Survey. Gilbert (1893) reviewed the characteristics of lunar craters and of various types of terrestrial volcanic craters and concluded that the differences in form, and to a lesser extent differences in size, between lunar and terrestrial craters

were so great that a volcanic origin for the lunar craters seemed improbable. He did, however, recognize a possible analogy between the smaller lunar craters and terrestrial volcanoes of the maar type. With this as a point of departure, Gilbert proceeded to develop an impact hypothesis for the origin of the lunar craters, which was based on some acute telescopic observations of the Moon and upon laboratory experiments. Four authors of whom he was cognizant had preceded Gilbert with an impact hypothesis: the astronomer R. A. Proctor (1873, and 1878), who later abandoned the idea, according to Mary Proctor (1928, p. 83); the architect Meydenbauer (1877 and 1882); and the architect and the theologian, August and Heinrich Thiersch, son and father, who wrote under the pseudonym "Asterios" (1879).

Gilbert felt that the predominantly circular or nearly circular form of the lunar craters required special explanation under the impact hypothesis, as impacts at other than vertical incidence had produced elliptical craters in his experiments. To alleviate this difficulty he devised an ingenious "moonlet" theory in which the craters were assumed to have been formed by the infall or sweeping up of smaller satellites of the Earth. From the theory he obtained a frequency distribution for the angle of incidence with a mode at vertical incidence. The underlying assumptions of this theory foreshadow the Moulton-Chamberlain hypothesis of planetesimal accretion, and Gilbert pointed out this implication, though he refrained from developing it. One of the major contributions in Gilbert's paper is the recognition of a radiating system of linear topographic features surrounding Mare Imbrium, which he termed "Imbrium sculpture ". He considered the circular maria as simply the largest members of the whole class of craters. In the detailed application of the impact hypothesis to the explanation of various features of the lunar surface, Gilbert's paper is remarkably modern in viewpoint when compared with the papers of such latter-day authors as Baldwin (1949), Urey (1951), and Kuiper (1954).

But Gilbert's views were too advanced for his time, and they were soon attacked by the geologists Branco (1895, pp. 280–314) and Eduard Suess (1895). At the close of the 19th century the consensus among both geologists and astronomers was still firmly in favour of volcanic origin of the craters.

The principal lunar crater-forming processes advocated by geologists since 1900 may be roughly classified into four major categories, following the German writers: (1) *Blasenhypothese*—bubble or steam blast or volcanic explosion hypothesis; (2) *Vulkanhypothese*—volcanic hypothesis or, more strictly, the caldera hypothesis; (3) *Gezeitenhypothese*—

tidal hypothesis, and (4) *Aufsturzhypothese*—impact hypothesis. The first three categories may all be considered varieties of volcanic hypotheses and no sharp separation can be made between them.

The *Blasenhypothese*, conceived in its extreme form by Robert Hooke as the bursting of gigantic bubbles, supposes some form of violent escape of gas from the lunar interior. In a more realistic form the hypothesis involves simply a sudden release or explosion of steam or volcanic gas from some place beneath the lunar surface. In this form it has been applied to some or all of the lunar craters by Sacco (1907), Dahmer (1911*a*, 1911*b*, 1912, 1938, and 1952), and Mohorovičić (1928). The *Blasenhypothese* may also be considered to include the maar type of volcanism, which involves violent gaseous eruptions and will be described below in more detail. In this form it has been supported by Branco (1894 and 1915), Eduard Suess (1909), von Wolff (1914), F. E. Suess (1917), and many others.

Most supporters of the *Vulkanhypothese* compare the lunar craters with terrestrial calderas. On the one extreme the comparison is with calderas formed during violent eruptions, such as Krakatoa, and on the other extreme the comparison is with calderas formed simply by quiescent subsidence, such as the summit calderas of the Hawaiian shield volcanoes. Besides Branco, the elder and younger Suess, and von Wolff, the list of advocates of some form of volcanic hypothesis for the origin of most lunar craters includes Simoens (1906), Günther (1911), Krejčí-Graf (1928 and 1959), Forbes (1929), Matoušek (1924*a*, 1924*b*, and 1930), Spurr (1944), Sacco (1948), Escher (1949 and 1955), Viete (1952), von Bülow (1954 and 1957), Jeffreys (1959, pp. 372–377), and Green and Poldervaart (1960). European geologists, in particular, appear to favour some combination of volcanic hypotheses to explain the majority of lunar craters.

At the quiescent extreme, the *Vulkanhypothese* shares many features with the *Gezeitenhypothese* or tidal hypothesis, developed by Faye (1881), Ebert (1890), Hannay (1892), and Pickering (1903). Under the *Gezeitenhypothese* it is assumed that the Moon was once fluid except for a thin crust. Tides raised by the Earth's attraction are supposed to have fractured the crust, permitting a part of the fluid interior to flow out on the surface and then to recede again with the passage of the tide. A part of the fluid congeals on the surface with each high tide and a circular rampart is thus built up around each locus of outflow. Among geologists, this hypothesis was received with some favour by Eduard Suess (1895 and 1909), but has not been seriously considered by others, except to the extent that tides can trigger volcanic activity (Ower, 1929).

The *Aufsturzhypothese*, or impact hypothesis, which received its most important early development from Gilbert, has been supported by Wegener (1920, 1921, and 1922), Spencer (1937), Fairchild (1938), Daly (1946), Dietz (1946), and Quiring (1946) as well as many astronomers. F. E. Wright, who undertook the most extensive and painstaking investigations of the Moon of all 20th century geologists, recognized merits in both volcanic and impact hypotheses but appears to have leaned toward volcanism to explain most of the lunar craters (Wright, 1927, p. 452, and in press). Unfortunately, with the interruption of World War II, Wright did not live to publish the bulk of his results and conclusions. N. S. Shaler (1903) and E. H. L. Schwarz (1909) advocated impact for the origin of the circular maria but turned to volcanism and other mechanisms to explain the other craters. In later papers, Schwarz (1927 and 1928) developed a "torsion cylinder" hypothesis, the mechanics of which are somewhat obscure, for the lunar craters and certain terrestrial craters.

Many other ideas, which are hardly profitable to review from a geological point of view, have been advanced to explain the lunar craters, such as the "ice" or "snow" hypothesis of Ericsson (1886) and Peal (1886), and the "vortex" or "sun spot" hypothesis of Rozet (1846) and Miller (1898). The latter, which might also be called the "convection current" hypothesis, has been revived in a more sophisticated form by the astrophysicist J. Wasiutyński, (1946) and supposes a fluid moon in which there are internal currents or a fluid moon with a thin crust. Craters are supposedly formed over individual convection cells.

It should be noted that a hypothesis of the astronomers Tomkins (1927) and Marshall (1943), in which lunar craters are supposed to have formed by the quiescent opening or collapse of the summit of a dome raised over a laccolith or blister of molten rock, closely resembles von Buch's old "craters of elevation" theory for the origin of terrestrial craters. The so-called lunar domes with summit craters, cited by Marshall as formed in this fashion, probably have, as will be shown, more direct terrestrial analogues.

B. Terrestrial Crater-forming Processes

Terrestrial craters are formed by a wide variety of processes, but terrestrial craters of only two general classes closely resemble the majority of lunar craters: (1) the maar type of volcanic crater, and (2) meteorite impact craters. These two kinds of craters are sufficiently similar in gross external form to have frequently been confused, one for the other. In fact, a volcanic or cryptovolcanic origin has been

proposed for nearly every major impact structure recognized up to the last few years.

Although most proponents of the volcanic origin of lunar craters have considered terrestrial calderas as homologues of the larger lunar craters, the majority of calderas differ from most lunar craters in several important respects. Only the most important need be mentioned at this point. Most calderas occupy the site of the central part of a volcanic edifice; the floor of the caldera is commonly higher than the level of the terrain surrounding the edifice (Reck and others, 1936; Williams, 1941). Lunar craters, on the other hand, in which the floor is higher than the terrain surrounding the crater rim are extremely rare. This discussion will be restricted chiefly to terrestrial features that closely resemble lunar craters.

In thus limiting the discussion, a separation has been drawn between calderas and maars, but the separation is not everywhere clear-cut in the field. Some craters in Mexico, for example, which I consider to be of the maar type (Galbraith, 1959) have been referred to by Jahns (1959) as calderas. The distinction depends upon minor but perhaps critical differences in interpretation of the history and mechanics of the craters. Most crater-form depressions referred to as calderas are considerably larger than maars.

As used by most present-day volcanologists, the term caldera is applied to large, more or less circular depressions which have been formed by the collapse of the summit of a pre-existing volcanic pile, commonly a cone-shaped volcano. The caldera is usually formed at a late stage in the history of the volcano, and the collapse or subsidence of the summit is commonly, but not always, accompanied by violent eruptions. As defined by Williams (1941), the caldera is larger than any individual eruptive vent.

A maar, on the other hand, is opened by piecemeal spalling and slumping of the walls of a volcanic vent during most of the eruptive history of the volcano. The smaller fragments are entrained in outrushing gas and distributed far and wide around the crater; a low rim of ejecta is generally formed, which is repeatedly engulfed on the inner edge by the ever-widening crater.

It is, of course, possible to have a combination of various crater-forming processes operative at a single volcanic vent, and late stage collapse or subsidence is also a common event in the history of some maars. Therefore the classification of certain volcanic craters will necessarily depend on the somewhat arbitrary decision or personal preference of the investigator. It should also be noted that there is no unanimous agreement among volcanologists on the details of the

mechanics of calderas or of maars. The theory of Escher (1929 and 1930) for the Krakatoa caldera resembles the theory presented here for volcanoes of the maar type.

On one point, on the other hand, there is now nearly unanimous agreement among close students of calderas. A caldera is formed by subsidence rather than by ejection of the rocks from the space occupied by the surface depression. The association of violent awe-inspiring eruptions, atmospheric waves and sea waves, with the collapse of the Krakatoa caldera in 1883 led to the widespread popular misconception, bolstered by the Royal Society report (Judd, 1888) that the volcano literally blew its top off. But a simple inspection of the ejected debris shows that this did not happen (Verbeek, 1886; Stehn, 1929). Most of the ejected material consists of pumice—frothy glass formed from new magma. There are far too few fragments of the old lavas of which the volcano was built to account quantitatively for the volume of rock which disappeared from the summit of the volcano during the eruption. A similar situation exists for nearly every other caldera of the Krakatoa type for which quantitative estimates of the ejecta have been made (Williams, 1941; van Bemmelen, 1929).

It is highly improbable that any volcanic eruption, although it may be classed as "explosive" by volcanologists, can be likened to the detonation of high explosives. The volcanic process commonly called explosive is simply the rapid discharge of gas, usually through some pre-existing orifice or vent. When rapidly moving volcanic gas, accelerated along a conduit by a moderate pressure gradient (Einarsson, 1950), encounters the relatively static air above the vent, visible shock waves may be generated in the atmosphere (Perret, 1912). The noise is often deafening but, despite the auditory similarity to a chemical explosion, the volcanic mechanism, as will be shown, is basically different.

III. Maars

"Maar" is a German or Rhinelander word applied to a number of small lakes that occupy volcanic craters in the dissected plateau of the Eifel region of Germany. As used by the German cartographers and geologists, "maar" or "dry maar" has also been employed to designate other similar volcanic craters in the Eifel even though they are not occupied by lakes (Hopmann, Frechen, and Knetsch, 1956). The craters are circular to elliptical or somewhat irregular depressions excavated in the Eifel plateau. They range from 70 to about 1500 m in greatest diameter, measured from rim crest to rim crest, and from about 10 to about 200 m deep, measured from the highest point on the rim to

the lowest point in the crater. Most of the craters are partially encompassed by an inconspicuous low ridge of ejecta composed partly of volcanic ash and lapilli and partly of pieces of pre-existing non-volcanic rocks from which the crater and underlying vent have been excavated.

The term "maar" or "maar-type volcano" has been very generally applied to volcanic craters scattered around the world which are similar to the German maars. Cotton (1952, pp. 258–267) has proposed the term "ubehebe" for the dry maar and "tuff ring" for the maar encircled by a higher rim of ejecta than is found at the Eifel maars. Here they will all be referred to simply as maars.

A. Surface Features of a Maar

For purposes of detailed description it is appropriate to take the Zuñi Salt Lake crater of western New Mexico (Darton, 1905) because it resembles closely in gross form a number of lunar craters of larger scale. The crater is a depression in the moderately irregular surface of the southern part of the Colorado Plateau and is encompassed by a low rim like the Eifel maars (Fig. 1). In the central part of the floor of the crater is a shallow saline lake from which rise two small basaltic cinder cones. The crater is about 2000 m across and the surface of the lake lies about 50 m below the general level of the surrounding terrain. The rim of the crater, which is of uneven height, rises about 125 m above the crater floor.

The rim is formed of bedded ejecta resting on nearly flat-lying older rocks. Mixed pieces of sandstone, shale, limestone, basalt and old crystalline rocks are found in the ejecta as well as lapilli of basalt, which represent drops of lava thrown out of the crater as the rim was being built up. Some of the sandstone, shale, and basalt fragments have been derived from beds exposed in the walls of the crater, but other rock fragments have been derived from considerably greater depth. The outer slopes of the rim are smooth and mostly gentle; the maximum gradient near the crest is about 30° and at the outer extremity the rim merges imperceptibly with the surrounding countryside. The deposit of ejecta thus forms a conical sheet which tapers gradually to a feather edge at the outer perimeter. In total volume the sheet would be insufficient to fill the crater, and the volume of pieces of rock in the sheet that are derived from the space occupied by the crater is a very small fraction of the volume of the crater.

The crater walls are irregular, steeply sloping surfaces underlain chiefly by sandstone and shale capped by the ejecta sheet of the rim. A basalt flow beneath the ejecta crops out as a low cliff on one side

FIG. 1. Zuñi Salt Lake, New Mexico; a maar with central cinder cones. Photograph by John S. Shelton.

of the crater. Sandstone, shale, and basalt, together with parts of the ejecta sheet, have dropped into the crater in a series of fault blocks (not described by Darton) along the west side, locally forming a series of terraces. The detailed features of the walls have been sculptured by erosion.

The crater floor is built up of coalescing small fans of alluvial detritus, derived by erosion of the walls and, in the centre, lake beds of undetermined thickness. The cinder cones, which represent the latest phase of volcanism at the crater, have been built upon the lake beds and rise to heights of about 50 m above the lake surface. A small crater in the centre of the largest cone descends to lake level.

Zuñi Salt Lake is a fairly representative maar, though the presence of cinder cones in the centre is unusual. Only one other maar with a central cone, the Wau en Namus of Libya (Viete, 1952, p. 475), has come to my attention. The Afton craters of southern New Mexico (Lee, 1907; Reiche, 1940) are more eroded and filled in than the Zuñi Salt Lake crater, but also exhibit the downfaulting or collapse along the crater wall. Well-developed bedding in the ejecta of the rim, which is a normal feature of maar rim deposits, led Reiche to interpret the beds in the largest of the Afton craters as fluviatile in origin. A decisive characteristic which shows such beds to have formed by fallout of ejecta, however, is the pronounced deformation of the beds under the larger blocks (Shoemaker, 1957). Such blocks in rare cases, such as in the rim of a maar in Puebla, Mexico (Ordoñez, 1905), are as much as 3 m across; the average grain size of the ejecta of maar rims commonly lies between about 5 and 10 mm.

Another feature of the bedding in the rim deposits that is characteristic of uneroded maars but also occurs at other volcanic craters is the draping of the bedding over the crest of the rim. This feature is well illustrated at several craters in Puebla. On the outer slopes of the rim the bedding is subparallel with the gently sloping upper surface of the ejecta deposit. Inward-dipping beds are found in some places on the inner slopes or walls of the craters as well. In general, the inward-dipping beds lie at angles close to the angle of repose of the material when it fell, ordinarily between 30° and 40°. Individual beds may be traced up the crater walls, over the crest of the rim, and down the outer slope. Generally only a thin layer of such beds, representing the last showers of ejecta, is draped over the rim crest. Lower beds in the rim deposit are most commonly truncated at the crater wall. The thin layer of inward-dipping ash or ejecta is quickly stripped away by erosion, but where preserved, it shows that the crater had attained nearly its final form prior to the last ejecta showers.

Draped bedding and inward-dipping ejecta may be found at the

Pulvermaar in the Eifel and the Cerro Colorado crater of the Pinacate region of Mexico (Jahns, 1959), but in these regions where the rim deposits are typically rather thin, the walls of the craters are more commonly bare bedrock. At the Diamond Head, Punch Bowl, and other maars on the island of Oahu, Hawaii (Stearns and Vaksvik, 1935), and at Crater Hill and other maars at Auckland, New Zealand (Firth, 1930), on the other hand, the walls of the craters are formed entirely of ejecta deposits. In these latter cases the floors of the present craters have been filled about to the level of the surrounding terrain or actually lie at a little higher level.

A crater of the maar type at Soda Lake, Nevada (Russell, 1885, pp. 73–76), has formed on the bed of the Pleistocene Lake Lahontan, after the lake had dried up. Fragments of the lake sediments, including shells of fresh-water invertebrates, are present in the ejecta of the crater rim. Evidently a similar occurrence of shells led Scrope (1862) to conclude that the maars of the Phlegraean fields in Italy were actually formed under water.

B. Subsurface Structure of Maars

In order to demonstrate the origin of maars it is necessary to know the relation of such craters to the underlying volcanic vents and to know the structure of the vents. One of the best places to examine these relations is in the Hopi Buttes region of the Navajo Indian Reservation, Arizona (Hack, 1942; Shoemaker, 1956; Shoemaker, and Roach and Byers, in press). Here some 300 maars of Pliocene age are well exposed in varying stages of denudation, more than are known in an area of comparable size in any other part of the world.

In the Hopi Buttes, the craters are found to be the surface features of funnel-shaped volcanic vents filled with a variable assemblage of blocks of old sedimentary rocks derived from the vent walls, basaltic tuff, tuff-breccia and agglomerate, fine-grained generally well-bedded clastic and carbonate rocks formed of sediments laid down in the craters, and intrusive and extrusive alkalic basalt. The vent walls generally slope gently (less than 45°) inward in the upper part where they cut soft Pliocene lake beds, and more steeply (more than 45°) where they cut well indurated Mesozoic rocks lower down. The walls cleanly truncate the older rocks, which are nearly flat-lying well-bedded sandstone and shale; the beds are deformed in only a few places. A volcanic vent with these characteristics has been called a diatreme by Daubreé (1891), who coined and applied the term to closely similar vents in Scotland and Germany as well as to the kimberlite pipes of South Africa.

Some of the diamond-bearing kimberlite pipes of South Africa, which are slightly different but closely related to the Hopi Buttes diatremes, have been completely explored by mining over vertical distances of

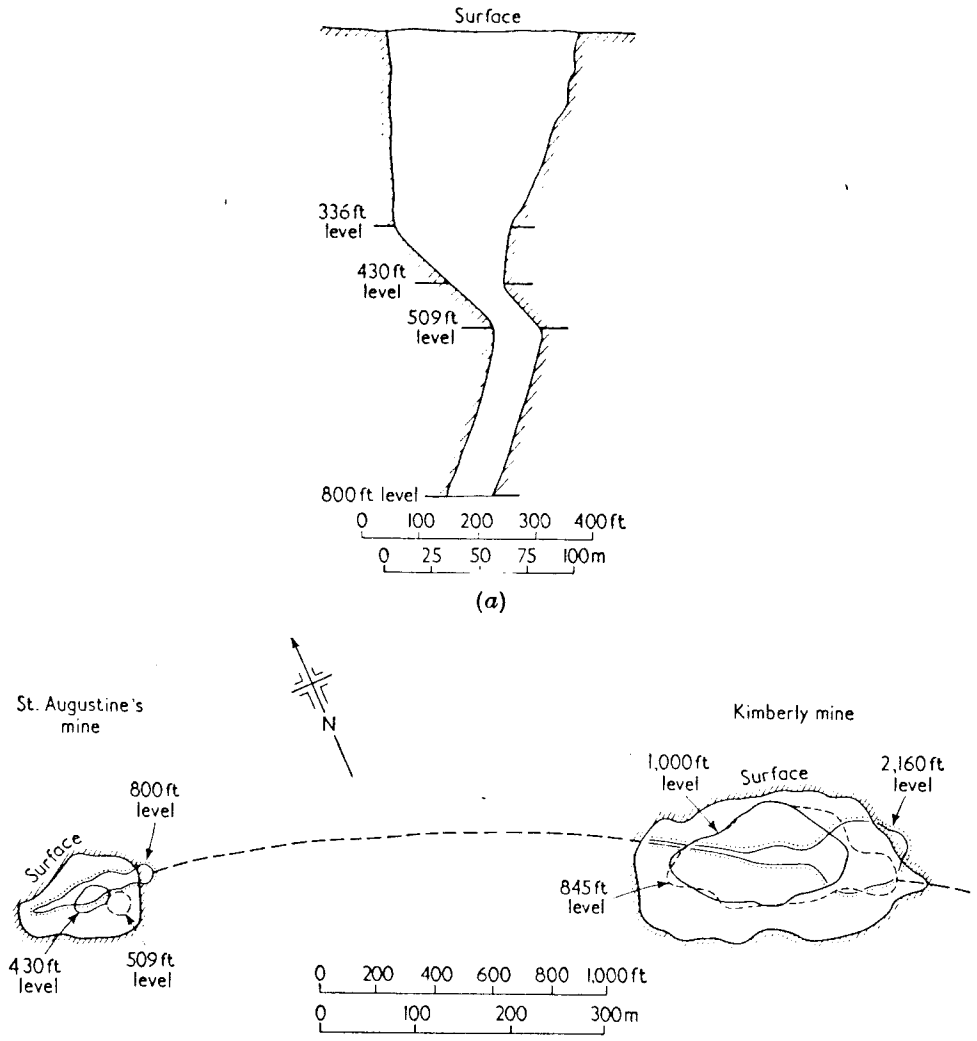

FIG. 2. St. Augustine's and Kimberley Mines, South Africa. (*a*) Section through St. Augustine's pipe in a northwest direction (after Wagner, 1914). (*b*) Plan showing contours of Kimberley and St. Augustine pipes (after Wagner, 1914).

more than 500 m (Fig. 2). They taper gradually downward into bodies increasingly elliptical in plan with depth; at the greatest depths reached by mining some pipes are elongated to dike-like forms. Kimberlite (serpentine breccia) diatremes of the northern part of the Navajo

Indian Reservation, which are exposed at a deeper level of erosion than the diatremes of the Hopi Buttes, exhibit a variety of forms at depths of several hundred to about 2000 m below the surface of eruption (Fig. 3). They range from mere local enlarged openings along dikes, as at Red Mesa (Fig. 3), to irregular pipe-like bodies with complex internal structure as at Mule's Ear (Fig. 3). These diatremes, at the level at

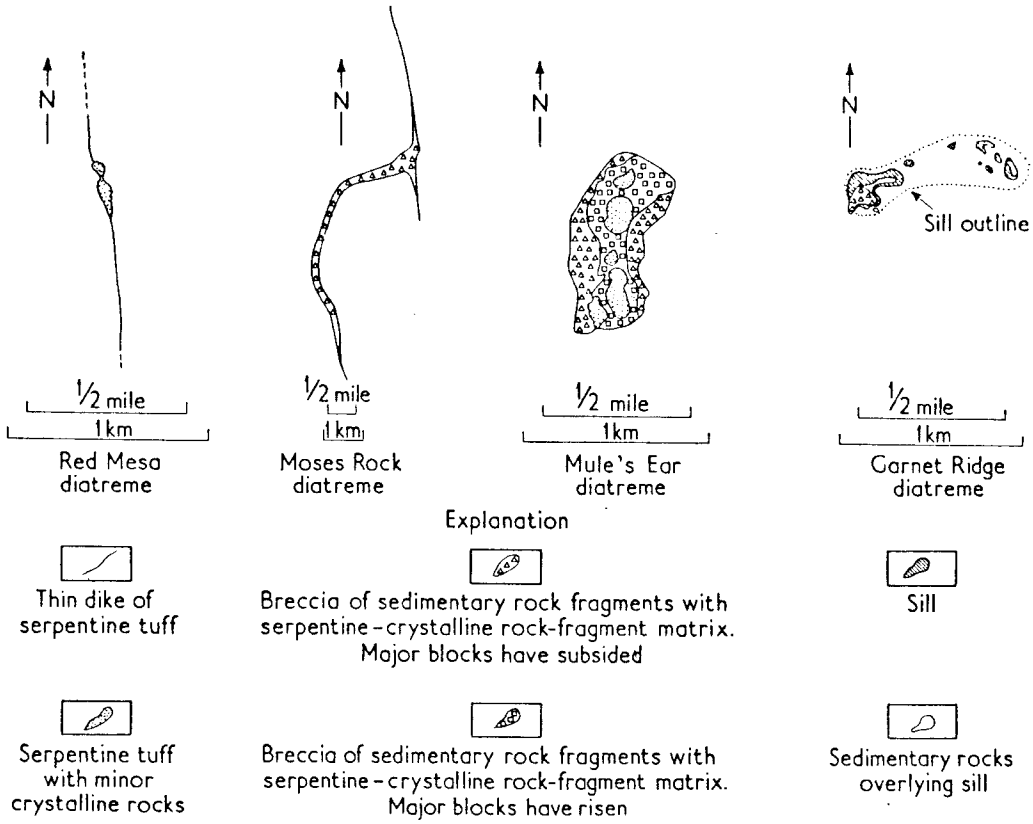

FIG. 3. Diagrammatic plan views of four serpentine-bearing diatremes in the northern part of the Navajo Indian Reservation, Arizona.

which they are exposed, are filled entirely with fragments of serpentine, ultrabasic rocks, and pieces of rock derived from the vent walls. Blocks of sedimentary rocks, some more than 40 m across, have dropped down the vent from the horizons at which they were derived, in places as much as 1500 m. Other pieces, generally much smaller in size, have come from great depth, some probably from below the Earth's crust. Pieces that have gone down are intimately mixed with pieces that have come up, but in the Mule's Ear diatreme the largest pieces that have gone down are concentrated along the wall of the vent and the center is filled mainly with pieces that have come up. The general mixing of fragments from different sources is a common feature of diatremes.

C. Mechanics of Maar-forming Eruptions

One of the few maars that has been observed in eruption and reported in the literature is the Nilahue maar, which was opened up in the Riñinahue volcanic field of southern Chile during the summer of 1955 (Müller and Veyl, 1957).

The entire eruptive history at Nilahue spanned about 3½ months. The initial volcanic activity consisted of violent gaseous discharges of about 20 to 30 minutes' duration interrupted by periods of complete quiescence. The duration of the gas discharges and intervening quiescent intervals gradually became longer during the life of the volcano. Ejecta, consisting mainly of new lava and subordinate pieces of older rock, were carried to heights of about 5 to 8 km by the gas discharges and showered down over an area extending more than 200 km from the volcano.

Stratigraphic relations of the ejecta of other maar-type volcanoes suggest that most of them are similarly short lived.

Steam clearly plays an important role in maar formation but there is no agreement as to the source of the water and the steps in its transformation to the gas phase. Some volcanologists, such as Stearns (Stearns and Vaksvik, 1935, pp. 15–16), have emphasized the importance of ground water in maar formation. There seems no reason to doubt that ground water has played the key role in rare "explosive" eruptions at Kilauea, Hawaii (Jaggar and Finch, 1924; Stearns, 1925), and possibly in the formation of Hawaiian maars and in other unusual eruptions as at Tarawera, New Zealand, in 1886 (Smith, 1887; Thomas, 1888). On the other hand many maars, such as those of the Eifel and Hopi Buttes, are associated with alkalic basalts that are characteristically rich in water and other volatile rock constituents. The gas phase given off in the eruptions at these craters may have been derived chiefly, if not entirely, from the basaltic magma. Here we will examine the eruptive mechanism for a magma that is saturated with volatiles at the onset of eruption. This is probably the only case that will have application to lunar craters.

The initial stages of opening of a maar-producing vent can only be inferred. Suppose that a magma rich in dissolved volatile constituents is ascending through the Earth's crust along pre-existing fractures or along new fractures propagated by the intruding magma. The events that will take place will be controlled by the vertical pressure gradient in the crust, which in turn is a direct function of the superincumbent load of rocks. For simplicity of discussion the rock pressure will be taken to be hydrostatic. The ascending magma ultimately reaches a level where the rock pressure is equal to the partial vapour pressure

of the magma. Exsolution or boiling of gas should begin in the magma intruded above this level.

One of the mechanical properties of rocks which is important to the next stage of the maar formation process is their very low tensile strength. Tensile fractures may be propagated in rocks by fluids moving along them under pressures only slightly exceeding, or in some cases even less than, the lithostatic or overburden pressure (Odé, 1956; Hubbert and Willis, 1957). This fact is well known from the practice of hydraulic fracturing to increase oil recovery in certain oil well operations. Depending on the supply and viscosity of the fluid, the fractures may be propagated very rapidly. If sufficient gas were evolved from a boiling magma to transmit pressure from the magma to the overlying regions of lower rock pressure, a fracture could be propagated up the lithostatic pressure gradient to the surface. Through this fracture the gas could then escape. During the initial propagation of the fracture there is a slight overpressure on the walls which forces them apart, but once the fracture is opened to the point where the gas begins to move along it at appreciable velocity there is actually a drop of pressure from the rock in the wall to the moving fluid.

Turning now to the upper tip of boiling magma, if the gas is drained rapidly away up the fracture, there will be a drop in pressure on the upper surface of the magma or at the level where froth or bubbles are beginning to form in the magma. A decompressional wave will therefore be propagated down the column of magma which will permit boiling to occur in a lower level in the magma column. If the gas exsolves sufficiently rapidly so that the formation of bubbles keeps pace with the wave front, the conditions of wave propagation would be somewhat analogous to those for deflagration waves in burning gases. Material would be accelerated upward, in the direction opposite to the propagation direction of the decompressional wave, at a velocity governed by the pressure difference across the wave front. Boiling would descend to the depth where the pressure on the low pressure side of the wave front just equals the vapor pressure of the magma. The physical condition of the material on the low pressure side of the wave front would be complex and probably would change rapidly as it moves up the vent. The bubbles would expand as the froth moves into regions of ever decreasing pressure, ultimately coalescing to form a gaseous continuum with entrained bits of partly degassed magma.

Decompressional waves would also be propagated into the walls of the fracture and the walls of the boiling part of the magma column, permitting rock to spall and become entrained in the moving gas-liquid system. The entire gas-liquid-solid melangé can be described as a

complex fluidized system (Matheson and others, 1949). Depending on the velocity and density of the system, individual particles may either rise or sink or maintain their level in the vent. Some initial widening of the vent probably takes place by simple abrasion of the walls by the entrained debris, but spalling (plucking) is probably the main process which opens the fracture along a channel which soon localizes most of the flow. Along the length of the channel the pressure drop across the walls will tend to be greatest where the channel is narrowest (Venturi effect). At great depth the spalling may be sudden and violent, as in the case of rock bursts in deep mines, but near the surface it may be a more gentle slumping. By these processes the vent is cored out, probably much after the fashion of the gas coring observed by Perret (1924, pp. 62–69) in the 1906 eruption of Vesuvius.

Periodicity in the gas discharge, such as was observed at Nilahue, could be due to a number of causes. In the simplest case, a periodic discharge would occur if there were a continuous slow upwelling of magma uniformly charged with dissolved volatiles. Each time the top of the fresh magma reached a certain critical level, boiling would begin. The upper part of the column would be removed as a fluidized system, after which the vent would be choked with the unexpelled debris. The whole repetitive mechanism may be similar in some respects to that of a geyser.

The simplest maars are the orifices of vents opened by gas-coring. The floors of the craters, initially, are formed by the debris left at the end of the last eruption. Most of the material expelled from the vent is carried so high by the high velocity jet of gas that it falls far from the crater, but a small fraction falls locally to form an ejecta deposit on the rim. The lower the velocity of the gas jets, the higher is the ejecta deposit of the rim.

The distribution of ejecta around the crater follows a probability function governed by the variable velocities and characteristics of successive jets, atmospheric winds, the frequency distribution of grain size, drag coefficients of the ejecta, and many other factors. The ejecta form a blanket-like deposit with diffuse margins and an original upper surface that is generally smooth down nearly to the scale of the individual fragments. Fragments from all sources in the vent are generally indiscriminately mingled in the ejecta.

In many of the Hopi Buttes maars, particularly the larger ones, the gas-coring phase of the volcanic activity was followed by a period of subsidence or withdrawal of material down the vent. Thick deposits of fluviatile and lacustrine beds were laid down in places on the subsiding vent debris and some of the craters were greatly enlarged by

slumping of the crater walls. The causes of the subsidence are not fully understood but are probably related to the presence of a fluid column of magma occupying the vent at depth. In about half the Hopi Buttes maars the volcanic activity culminated in the quiescent upwelling of lava that filled the craters and commonly piled up to form low lava domes, in some places spilling over or cutting through the ejecta rims to form short flows.

D. Possible Maars and Other Volcanoes on the Moon

A nearly universal feature of maars, where they occur in considerable number as in the Eifel and the Hopi Buttes, is their tendency to be aligned in chains or rows. In the Hopi Buttes, dikes may be found in places between the craters, but more commonly there is no geologic feature connecting the craters along a given row at the surface. The alignment is probably due to some major fissure at depth along which the magma rose. In some places this fissure may be an old structure in the Earth's crust; in others the fissure may have been propagated by the magma itself (Anderson, 1951, pp. 22–28).

On the Moon, chains of small craters are common; most writers have supposed them to be of volcanic origin. There appear to be several different types of crater chains which should be examined separately.

A row composed of both small individual craters and small domes in the centre of Hell plain, pointed out by Alter (1957, p. 249), is similar to the chains of craters and domes of the Hopi Buttes, but is of slightly larger scale. Individual craters and domes are as much as 4 km across and are spaced from about 1 to 10 km apart. The entire chain, which forms a smooth arc, is more than 100 km long; in the Hopi Buttes, individual craters and domes are rarely more than 2 km across and the identifiable crater chains are not more than about 20 km long. The relative relief of the craters and domes on Hell plain, though not precisely known, appears to be comparable to the Pliocene relief in the Hopi Buttes. No visible surface features appear to connect the craters and domes in this chain on Hell plain, but higher resolution than has been achieved to date might reveal some.

A frequently cited chain of craters extending northeast of Stadius, between Copernicus and Eratosthenes (Fig. 4), appears to be of a slightly different type. The interpretation of this crater chain is complicated by the presence of numerous other small craters in the vicinity which are directly related to the large crater Copernicus. Craters that appear to belong strictly to the chain range from about 3 to 5 km across. Some occur individually, but most are adjacent to

or merge with other craters in the chain. At the north end, a line of contiguous craters passes northward into a rill, a long narrow trench. These craters are characterized by a distinct rim rising above the surrounding terrain except on the sides on which they are contiguous with other craters. They are staggered somewhat irregularly along the curving course of the chain over a distance of about 130 km. This chain might be compared with the chain of craters extending from Daun to Bad Bertrich in the Eifel. Again the scale of the lunar craters is somewhat larger. None of the craters in the Eifel chain much exceeds 1 km in diameter and the whole chain is only about 18 km in length.

Lunar rills, with which some crater chains are associated, may not have any close terrestrial counterparts. It is likely, however, that the original surface features associated with the Moses Rock diatreme (Fig. 3) resembled the cratered rill at the north end of the Stadius chain or, to take an example at a larger scale, the great Hyginus cleft (Fig. 5). A major crater was probably located above the sharp bend in the Moses Rock diatreme just as the crater Hyginus occurs at the bend in the great lunar cleft. The Hyginus cleft, however, is about 15 times larger than the Moses Rock diatreme and associated dike system. A closer analogy may exist between the Moses Rock diatreme and some of the Triesnecker rills (Fig. 5). Both the diatreme and Triesnecker rills show branching. Some of the broader lunar rills or clefts, such as Hyginus and the nearby Ariadeus rill, may be complex structures that are part diatreme and part graben. Perhaps the closest terrestrial homologues of the narrower rills are the Icelandic *gjá*, great fissures in the lava fields, some of which are tens of kilometres long.

Certain small craters along rills in the floor of the large lunar crater Alphonsus are surrounded by diffuse dark haloes extending out 4–5 km from the edges of the small craters. The occurrence of these craters along the rills shows that they are probably related to processes that have taken place within the Moon. They are of the form and size of ordinary terrestrial maars and the dark haloes may well be thin deposits of dark volcanic ash.

A number of similar dark halo craters are scattered individually in the region around Copernicus (Fig. 6) and a few occur near Theophilus. These may correspond to isolated terrestrial maars such as Zuñi Salt Lake. The largest crater with a dark halo, which occurs south of Copernicus and west of Fauth (Fig. 6), is about 5 km in diameter. In all cases the dark halo is nearly symmetrically distributed about the crater and has a diffuse outer margin.

Other features in the vicinity of Copernicus resemble other types of terrestrial volcanoes. A number of well-known symmetrical hills rising from the Oceanus Procellarum near its western edge, just north of Hortensius (Fig. 6), have been referred to in the astronomical literature as domes. They are about 7–9 km across, a few hundred metres high, and most have a small crater, less than 1 km in diameter, in the summit. In all discernible respects they appear to be small shield volcanoes, as was concluded long ago by Pickering (1906, p. 156–157), who discovered the first such object in the Mare Nubium. Many similar objects have been noticed by Kuiper (1959*a*, p. 308–309), and others in parts of the Oceanus Procellarum between Copernicus and Kepler.

Midway between Hortensius and Copernicus (Fig. 6) is another symmetrical hill, about 5–6 km across and at least several hundred meters high, with a conspicuous crater more than 1 km across in its summit. This feature resembles a small stratovolcano. It is perhaps the best example of its type to be seen in the subterrestrial hemisphere of the Moon. Other hills with summit craters are known, but their origin may be more complex.

The largest craters that occur along well defined chains are about 15 km in diameter.† Hyginus, which is 10 km in diameter, is one of the largest. Perhaps the largest occurs in a spectacular chain just northwest of Almanon. These craters have the approximate shape of maars, but if they occurred on Earth they would probably be referred to as calderas simply because of their large size. The largest terrestrial craters that I consider to be maars are about 5 km in diameter.

The great majority of lunar chain craters of the types described are similar in size to most terrestrial maars. Many are close to the limit of resolution in existing good lunar photographs (about 1 km in diameter). All of the lunar forms that resemble terrestrial shield and stratovolcanoes are of moderate dimensions, and most are perhaps slightly smaller than the average for their possible terrestrial counterparts. These facts suggest that volcanic processes, and in particular crater-forming volcanic processes, have operated on about the same linear scale on the Moon as on the Earth.

† The question of what constitutes a chain will be left in abeyance here. A straight or curved line may be drawn through any two craters, and among the thousands of visible craters on the Moon there must be a large number of instances where three or more craters are approximately aligned as a result of a fortuitous combination of unrelated causes. Calculation of the probability that any particular arrangement of craters may occur by a chance combination of certain events necessarily entails *a priori* assumptions, the validity of which are not readily tested. It must be remembered that finding any specified arrangement of craters is, *a priori*, highly improbable.

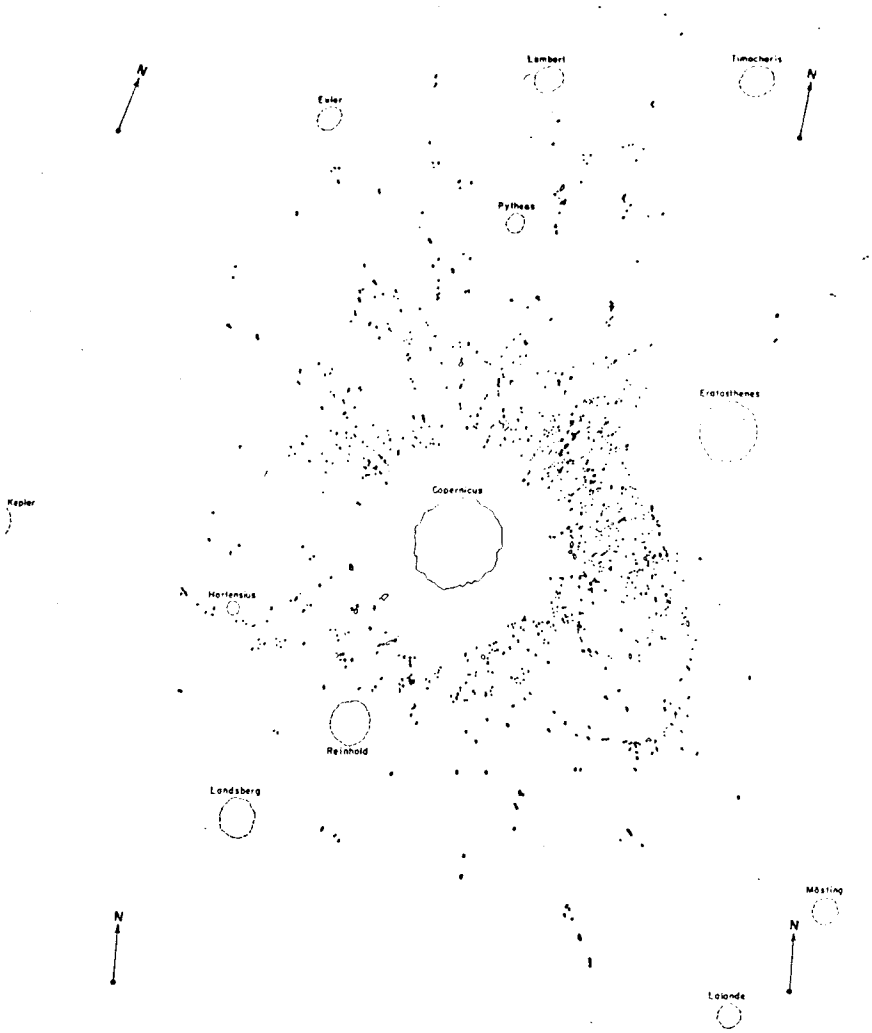

FIG. 4(*a*). Secondary impact craters of the Copernican ray system.

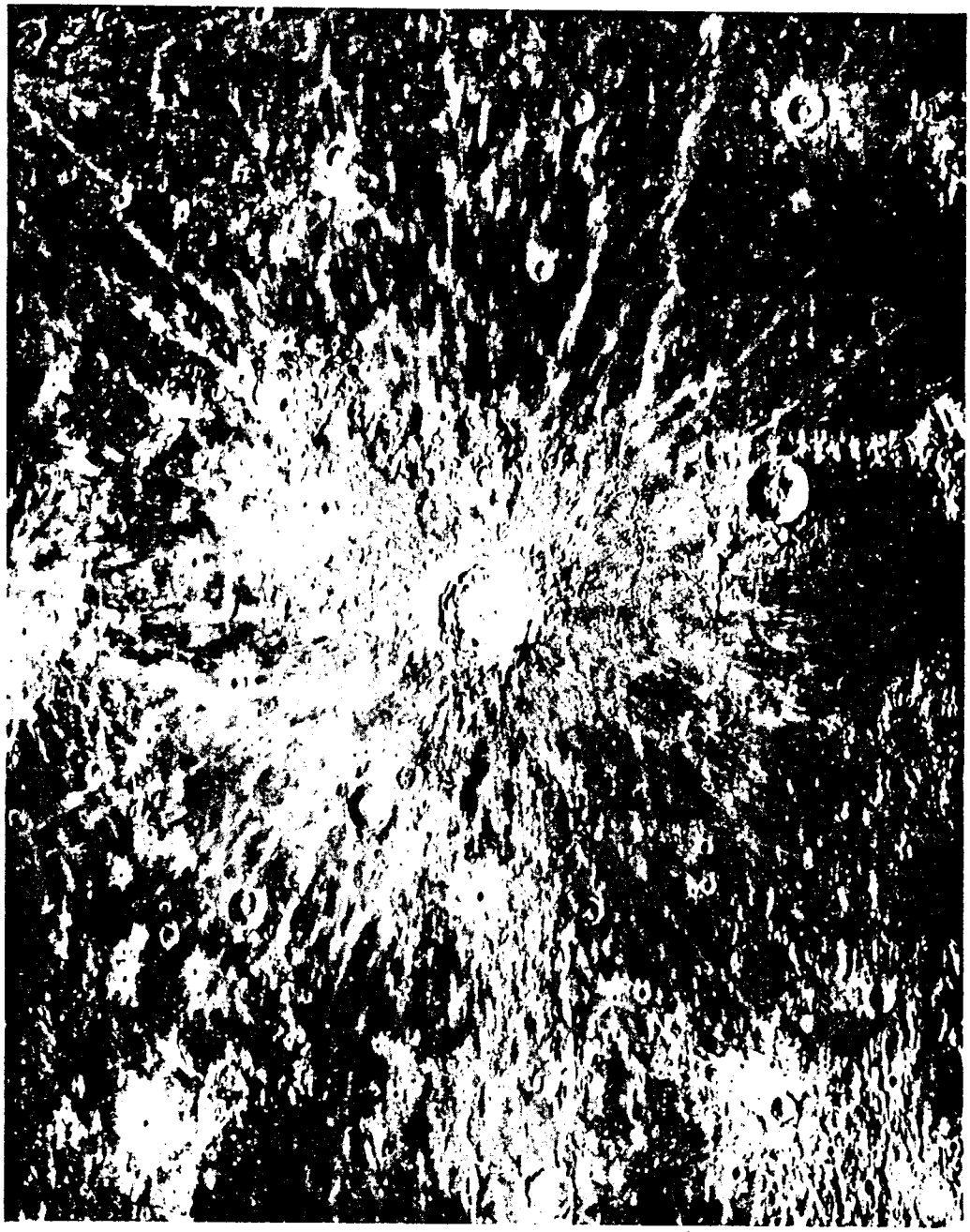

FIG. 4(*b*). Base photograph of the Copernicus region taken by F. G. Pease with the 100-in Hooker telescope in 1929, Mount Wilson Observatory.

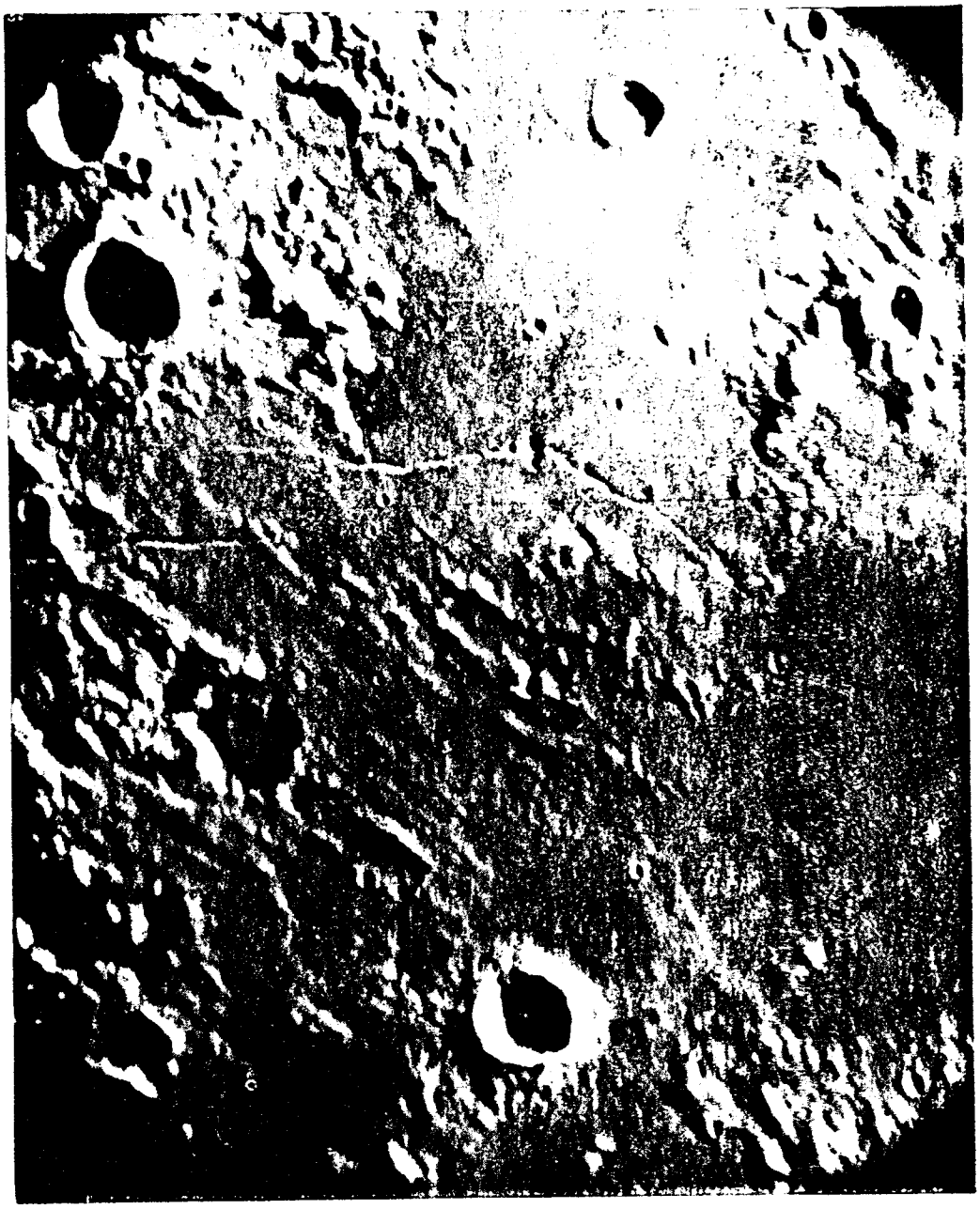

FIG. 5. Photograph of the Hyginus region of the Moon. (Observatoire du Pic-du-Midi).

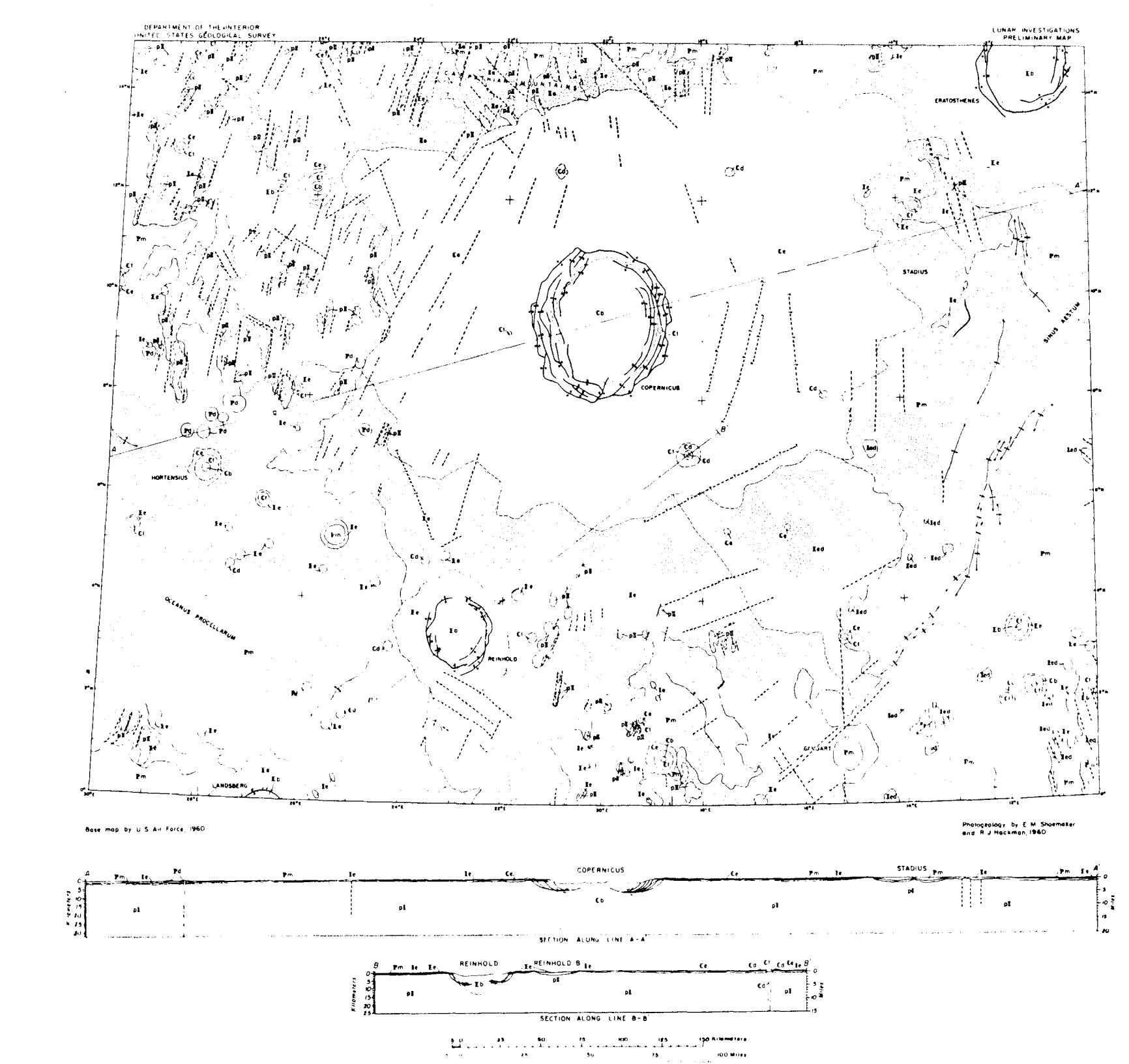

FIG. 6. Preliminary photogeologic r

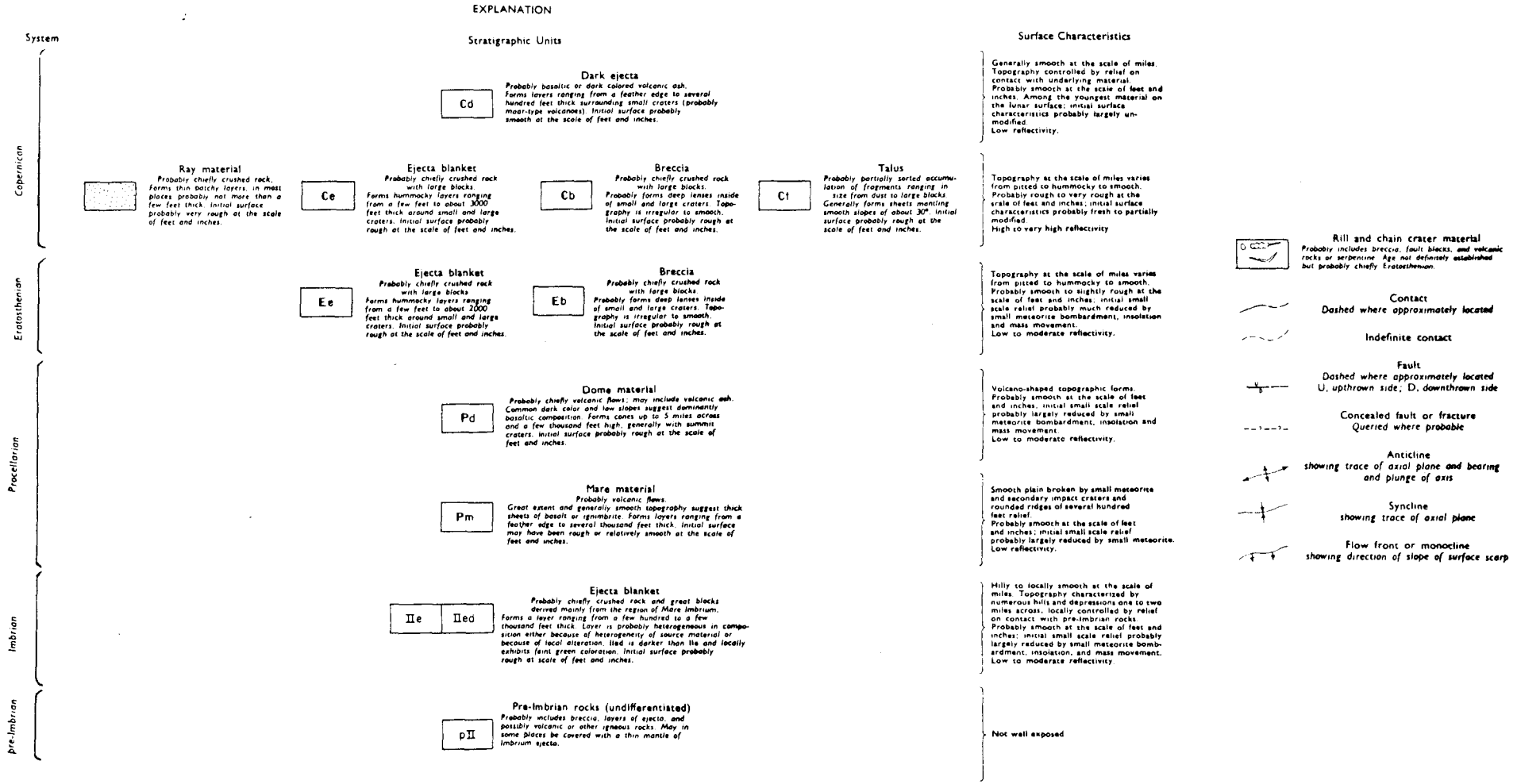

FIG. 6. Preliminary photogeologic map of the Copernicus region of the Moon.

[facing page 306]

IV. Impact Craters

The list of terrestrial craters of probable impact origin (Spencer, 1933; Boon and Albritton, 1938; Leonard, 1946; Hardy, 1954) now grows at the rate of about one a year (for some recent additions to the list see Karpoff, 1953; Beals, Ferguson, and Landau, 1956; Beals, 1958). Additions to the list fall into two categories, (1) previously undescribed craters, and (2) previously known craters for which evidence of impact origin has been found or for which such evidence has been strengthened. The growth of this list is likely to continue, perhaps to accelerate. Meteorite impact, however, has not yet been generally acknowledged as a process capable of or responsible for the formation of Earth features of more than modest size and number. This fact, as much as any other, has profoundly influenced past discussions of the origin of the craters of the Moon. The process of recognition of impact craters, therefore, begins on the Earth.

A. Form and Structure of Impact Craters

The best known and first widely recognized meteorite impact crater in the world is Meteor Crater, Arizona.† The crater occurs in a region underlain by nearly flat-lying sedimentary rocks of contrasting lithology, and it has been possible to determine the structure of the crater in detail (Shoemaker, 1960*a*, and in press). For this reason it is appropriate to use Meteor Crater, Arizona, as an example for detailed description and analysis.

Meteor Crater lies in the southern part of the Colorado Plateau in an area of low relief and generally excellent exposures. The crater is a bowl-shaped depression 200 m deep, a little over 1 km wide, encompassed by a ridge or rim that rises about 30–60 m above the surrounding plain. As computed by Gilbert (1896, p. 9), the volume of the rim will just fill the depression. The rim is composed of rock debris and alluvium resting on disturbed dolomitic limestone, shale, and sandstone strata. Beds exposed in the walls of the crater include, in ascending order, light coloured sandstone and dolomite of Permian age, and red sandstone and mudstone of Triassic age. The debris of the rim has been found by mapping to be rudely stratified as well; each mappable stratum is composed chiefly of fragments from one of the underlying formations and the fragmental strata lie in a sequence the inverse of that of the underlying formations from which they are derived (Fig. 7). Pieces of rock making up the debris range in size

† Meteor Crater, Arizona, has been named the Barringer Meteorite Crater by the Meteoritical Society in honour of D. M. Barringer, who contributed most heavily in establishing the impact origin of the crater.

from microscopic splinters to great angular blocks more than 30 m across.

The surface of the surrounding part of the Colorado Plateau has been eroded since Meteor Crater was formed, and in the vicinity of the crater has been lowered, on the average, about 15 m. In most places,

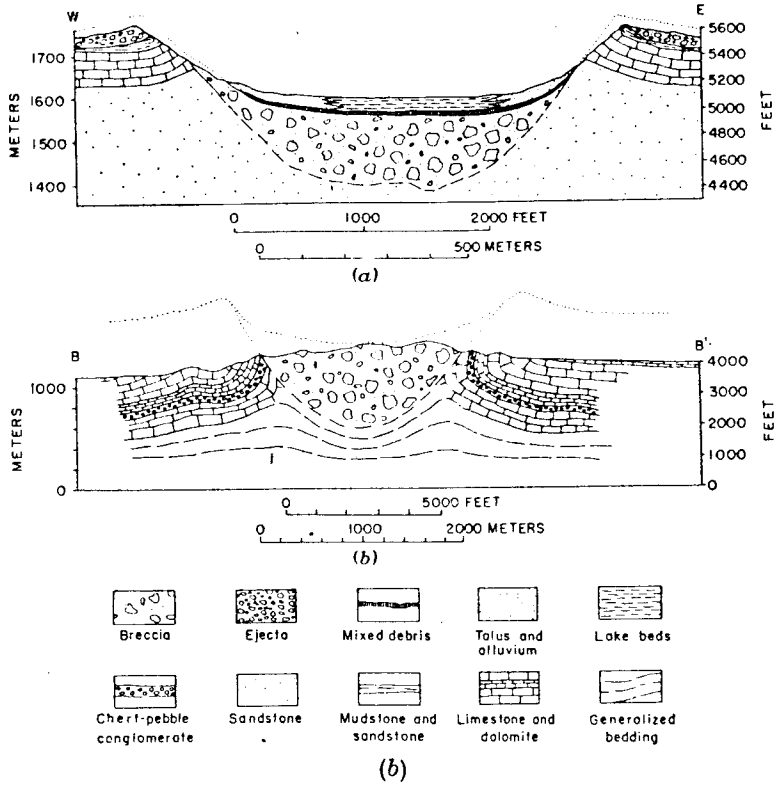

FIG. 7(*a*). Cross sections of Meteor Crater, Arizona, and (*b*) Sierra Madera, Texas.

the debris has been stripped down to a resistant layer formed by fragments of dolomite. Thin patches of late Pleistocene and Recent alluvium, composed mainly of detritus derived from the debris, rest on this stripped surface. The initial features of the crater rim, therefore, are not preserved, but the present topography of the rim affords important clues to its original appearance (Fig. 8). Today it has a peculiar hummocky rolling surface and it is likely that the original surface of the debris was similarly hummocky. Beyond a distance of about 1 km from the crater only scattered isolated fragments of debris remain.

Beds of the older formations exposed in the crater walls dip gently outward low in the crater and generally more steeply outward close to the contact with the debris of the rim. Along the north and east

FIG. 8. Meteor Crater, Arizona; an aerial view from the southeast. Photograph by John S. Shelton.

walls of the crater the uppermost red beds locally are folded back on themselves, the upper limb of the fold consisting of a flap that has been rotated in places more than 180° away from the crater (Fig. 7). At one place the flap grades outward into debris. Rocks now represented by the debris of the rim have been peeled back from the area of the crater, somewhat like the petals of a blossoming flower.

The upturned strata are broken by small nearly vertical faults of scissors type of displacement and a number of small thrust faults. Displacement on the vertical faults generally increases towards the centre of the crater. Regional jointing has controlled the shape of the crater, which is somewhat "square" in outline; the diagonals of the "square" coincide with the trend of two main sets of regional joints. The largest vertical faults, which are parallel with the regional joints, occur in the "corners" of the crater. Along one side there are also a few inward-dipping normal faults concentric with the crater wall.

The floor of the crater is underlain by talus and alluvium that interfinger toward the centre with lake beds about 30 m thick. These sediments rest, in turn, on a layer of mixed debris about 10 m thick that appears to have been formed by fallout of ejecta thrown to great height. The debris is composed of mixed fragments of the older sedimentary formations, some highly sheared and sintered, and contains sparse oxidized meteoritic iron. Though this layer apparently has not been preserved outside the crater, similar materials occur in the alluvium and as lag on the rim.

Beneath the mixed debris layer is a lens of breccia about 200 m thick, which has been partly explored by shafts and by about two dozen deep drill holes sunk by Barringer and his associates in the central part of the crater (Barringer, 1905, 1910, 1914; Tilghman, 1905). Along the upper outer margins of the lens the breccia is composed chiefly of large blocks of dolomite, but under the central part of the crater floor the breccia is made up chiefly of shattered twisted blocks of light-coloured sandstone and subordinate finer grained pieces of sheared and sintered rocks. The dolomite blocks of the upper edge of the breccia lens have been displaced downward against the sandstone in the crater walls. Meteoritic iron is dispersed in the breccia chiefly as microscopic spheres in drops of sintered dolomite, which appear to be most abundant near the base of the breccia. The sintered material constitutes not more than a few per cent of the breccia.

Recently the new mineral coesite, which had previously been known from the laboratory, has been found to be a major constituent of some of the sheared and sintered rock fragments at the crater (Chao, Shoemaker, and Madsen, 1960). Coesite is a dense polymorph of silica

which has been synthesized only under hydrostatic pressures exceeding 20,000 atmospheres (Boyd and England, 1960). Its occurrence at Meteor Crater is evidently the result of strong shock such as would be generated by hypervelocity impact. Coesite-bearing fragments occur in the breccia lens, in the layer of mixed debris interpreted as fallout, and also in the alluvium on the crater rim.

A small meteorite crater about 200 m across, the largest of a group of small craters near Odessa, Texas, exhibits structural features differing from those found at the Arizona crater (Hardy, 1953). The Odessa crater has been formed in nearly flat-lying Cretaceous beds of the Edwards Plateau (Sellards and Evans, 1941). In the walls of the crater these beds are buckled in a tight asymmetric anticline. Under the centre of the crater is a lens of fragmented and pulverized rock that appears to correspond to the breccia lens at Meteor Crater, Arizona.

Prior to exploratory excavation, the Odessa crater had been nearly obliterated as a topographic feature by erosion of the rim and filling of the central part with about 30 m of Pleistocene and Recent sediments. The general erosion of the plateau surface since the crater was formed is about the same as at Meteor Crater, Arizona. Both features are of late Pleistocene age. The meteoritic material at the Odessa crater is closely similar to the ordinary Canyon Diablo irons of the Arizona crater (Lord, 1941; Beck and La Paz, 1951), and it may be that the meteorites that formed each crater are part of the same fall.

The largest terrestrial crater for which there is now strong evidence of impact origin is the Ries basin or Rieskessel of southern Germany. It is a broad shallow basin between the Schwäbian and Franken Alb that has attracted the attention of the German geologists for well over 100 years. The idea that the Ries might be an impact crater was first set forth by Werner (1904) and later elaborated by Stutzer (1936). But the consensus of the principal investigators of the Ries, as summarized by Dorn (1948), has been that the Ries was formed by some sort of volcanic explosion.

The Ries basin or crater is of mid-Tertiary age and has been greatly modified by erosion and sedimentation. Originally the crater measured about 27 to 29 km from rim to rim. Miocene lake beds up to 300 m thick have been deposited on the crater floor (Reich and Horrix, 1955). Present maximum relief between the centre of the basin and the southern rim is about 200 m and the original relief must have been more than 500 m. The original topography within the crater comprised a central depression about 12 km across, now filled with sediments, surrounded by an irregular shelf from which rose scattered hills.

Breccias, chiefly of old crystalline rocks, are exposed on some of these hills where they rise above the floor of the Ries today.

The walls of the crater and crest of the rim (the *Schollen- und Schuppen-Zone* of Bentz, 1927) are underlain by breccia and an imbricate series of thrust sheets composed chiefly of Upper Jurassic limestones that cap the Alb (Nathan, 1925, 1935; Dehm, 1932; Gerstlauer, 1940; Schröder and Dehm, 1950; and Triebs, 1950). Beyond, extending tens of kilometres to the south in the region described by Branco (1902) as the *Vorries*, are great masses of limestone breccia resting on the undisturbed limestone cap of the Alb and, at the outer limit, on Oligocene sediments. One far flung fragment of limestone, measuring nearly half a metre in diameter, was found 60 km from the crater (Reuter, 1925). In places in the *Vorries* and the *Schollen- und Schuppen-Zone*, breccias composed chiefly of Lower Jurassic and Triassic sedimentary rocks or of rocks from the crystalline basement complex rest on the breccias of Upper Jurassic limestone and the thrust slices. Locally fragments of Triassic rocks and crystalline rocks are mixed in about equal proportion. Similar breccias were found in a deep drill hole under the lake beds near the centre of the Ries. Branco (1902) and later Bentz (1925) long ago concluded that the key to solving the origin of the Ries lay in explaining the mode of emplacement of these unusual breccias.

The most remarkable aspect of the geology of the Ries is a supposed volcanic breccia or tuff that has been called *suevit* (Sauer, 1901). It occurs both inside the crater and on the rim and *Vorries*. The *suevit* consists of a wide variety of rock fragments, most of them crystalline rocks from the basement complex, in general shattered or partially sintered, as well as bombs and smaller fragments of glass that all German authors have agreed are of a conventional igneous or magmatic origin. The glass bombs invariably carry fragments of sintered or partially sintered rocks that are recognizably derived from the crystalline basement. Some of the bombs have extraordinary shapes for volcanic ejecta such as thin sheets that have been tightly folded or curled on the edges. While this manuscript was in preparation some of the sintered material in the *suevit* was found to contain coesite (Shoemaker and Chao, 1960, Pecora, 1960, p. 19) and the Ries was thus established as the world's second locality for this high pressure polymorph of silica.

The *suevit* has been commonly assumed to have erupted from numerous widely scattered vents and, because the *suevit* can locally be seen to rest on the other breccias, the eruptions have been interpreted as one of the latest events in the development of the Ries. On the basis

of about a week's field study, I believe that the *suevit* can be interpreted to rest everywhere on the other breccias; local steep contacts of *suevit* with other breccia within the crater are probably due to faulting or inward slumping of the breccias along the crater walls. The sum of evidence indicates that the glassy material of the *suevit* has been fused by shock; the patches of *suevit* that have been preserved from erosion appear to be remnants of a layer that is analogous to the mixed debris or fallout layer preserved in Meteor Crater, Arizona.

Structurally the Ries is utterly unlike any caldera or crater of demonstrable volcanic origin. Indeed, *suevit* is the only material at the Ries that resembles volcanic rock. Kranz (1911, 1934) has attempted to explain the Ries in terms of one large volcanic explosion, but, as Reck has pointed out (Williams, 1941, p. 303), no masses of rock even approaching the size of the thrust slices of the *Schollen- und Schuppen-Zone* have ever been ejected in the most violent historic volcanic eruptions. To explain the thrust slices, a variety of complicated hypotheses have been invented that involve first an uplift or doming of the central part of the Ries and a later subsidence. All of the major structural features of the crater and the ejecta, on the other hand, appear to have a straightforward explanation in terms of hypervelocity impact mechanics.

A much smaller crater that has been generally agreed by Branco and Fraas (1905) and later workers to be closely related to the Rieskessel is the Steinheim basin. The Steinheim lies on the Schwäbian Alb about 30 km southwest of the Ries and is also partly filled with Miocene lake beds. Within the limits of error of paleontological dating the two craters are of the same age. The present Steinheim basin is about $2\frac{1}{2}$ km across and 80 m deep. It has been considerably modified by erosion and breaching of the crater rim by a through-flowing stream as well as by sedimentation on the crater floor. It is of interest as the only terrestrial crater so far recognized of probable or possible impact origin that exhibits a well-defined central hill. The walls of the crater are underlain by breccia of Jurassic limestone, and the central hill is underlain by highly disturbed but poorly exposed Jurassic rocks including some beds or rock fragments derived from lower horizons than any of the fragments in the breccia along walls. Branco and Fraas (1905) inferred that the Steinheim basin is an explosion crater of cryptic (hidden) volcanic origin; no direct evidence of volcanism is present at the crater. Exposures are not sufficient to determine how closely the structure of the Steinheim basin compares with that of demonstrated meteorite impact craters, but what is known of the structure is compatible with an impact origin. It seems possible, if not likely, that

the Steinheim basin was formed by impact of a part of a larger object, the main impact of which produced the Rieskessel.

B. Eroded Structures of Probable Impact Origin

A complex feature that may be interpreted as the subsurface structure of an ancient impact crater is well exposed at Sierra Madera, Texas, a hill, or small mountain on the southern edge of the Edwards Plateau (Fig. 7). This is one of a number of localities in the United States, exhibiting a community of structural features, that have been called "cryptovolcanic" (Bucher, 1936) or "cryptoexplosion" in origin (Dietz, 1959 and 1960). Boon and Albritton (1937, pp. 60–62) originally suggested that the structure at Sierra Madera was produced by meteorite impact, on the basis of mapping by King (1930, pp. 123–125). This suggestion has been considerably strengthened by information from three deep drill holes and by re-examination of the central part of the structure.

King mapped Sierra Madera as a complex dome with steeply dipping to nearly vertical and even overturned beds near the centre encompassed by partially concentric folds. The steeply dipping older rocks at the centre of the structure are found on close examination to be individual blocks in a lens of a giant breccia nested in a cup of peeled back and locally overturned beds (Fig. 7). A drill hole somewhat off of the centre of the breccia lens shows that, beneath the breccia, the structural relief on an anhydrite marker bed is only a few hundred feet.†

The age of the Sierra Madera structure is not known. Cretaceous as well as Permian beds appear to be deformed and a considerable thickness of Cretaceous rocks would be required to restore the crater suggested in Fig. 7. A pre-Pleistocene age seems required to account for the regional denudation since the structure was formed. In all probability the structure is of Tertiary age. Much more work needs to be done at Sierra Madera, and a detailed geologic study will probably increase the understanding of similar geologic features.

Other structures referred to as "cryptovolcanic" or "cryptoexplosion" structures have also been mapped as domes surrounded by concentric folds, but the exposures are rarely adequate to support this interpretation. The domes are inferred more from the fact that the oldest rocks are found near the centre than from observable field relations. The oldest rocks indeed are generally found near the centres of the structures, but where quarries have been opened up or drill core obtained, as at Wells Creek Basin, Tennessee (Wilson, 1953, pp. 766–768),

† I am indebted to Mr. Addison Young for identification and correlation of the anhydrite bed.

these rocks have turned out to be fragments in a breccia similar to that at Sierra Madera. Upheaval Dome, Utah, which was called cryptovolcanic by Bucher (1936, pp. 1064–1066), has a well-exposed broken dome in the centre, but this structure is probably a salt dome (McKnight, 1940, pp. 124–128; Joesting and Plouff, 1958) and not related to structures of the Sierra Madera type. Each geologic feature that appears to belong to the "cryptoexplosion" category must be examined on its own merits.

The largest known structure that appears to be of the Sierra Madera type is the so-called Vredefort "dome" of South Africa (Hall and Molengraaff, 1925; Nel, 1927) which is 70 to 90 km across. The centre of the Vredefort structure is also occupied by a great mass of brecciated rock. Boon and Albritton (1937, pp. 62–64) and later Daly (1947) suggested that the Vredefort structure was formed by impact, but South African geologists appear to prefer more conventional geologic interpretations of its origin (Brock, 1951).

C. Similarity between Impact Craters and Nuclear Explosion Craters

Most of the principal structural features of large meteorite impact craters are reproduced in one or the other of two craters formed by underground explosions of nuclear devices in alluvium of Yucca Flat, Nevada (Shoemaker, 1960*a*). Detonation of a 1·2 kiloton device at about 6 m depth produced a crater about 80 m in diameter and 15 m deep (the Jangle U experiment).† A device of the same yield detonated in the same medium at a depth of about 20 meters produced a crater about 100 m in diameter and about 30 meters deep (Teapot Ess experiment). Different structures were produced in the rims of the two craters but both are underlain by a lens of breccia.

The Teapot Ess crater is a fairly close model at about 1/11 scale of Meteor Crater, Arizona. Beds of the alluvium are turned up and overturned along the wall of the crater and ejecta fragments are stacked on the rim roughly in an order inverted from the order of the beds from which the pieces are derived. The Jangle U crater is approximately a half-scale model of the main meteorite crater at Odessa, Texas. Beds are buckled in an asymmetric anticline beneath the rim. The anticline is sheared off at the top and the crest of the rim is formed of large slabs of ejected alluvium. These slabs may correspond, on a small scale, to the great thrust sheets of the *Schollen- und Schuppen-Zone* of the Ries. The post-shot topography of the outer flanks of the rim of both the Jangle U and Teapot Ess craters was characteristically

† 1 kiloton is equivalent to 10^{12} calories or $4{\cdot}186 \times 10^{19}$ ergs total yield.

hummocky, resembling, on a small scale, the hummocky terrain on the rim of Meteor Crater, Arizona.

From the nuclear explosion craters it can be seen that the surface and structural features of impact craters can be produced by strong shocks originating at shallow depths beneath the surface of the ground and also that the structures formed depend upon the depth of the origin of the shock. Comparably strong shocks are produced by hypervelocity impact. It may be anticipated that the structure of large meteorite craters will depend upon the depth of penetration of the meteorite, the total energy released, and the nature of the target rocks.

It would be erroneous to conclude from the structural similarities to explosion craters, however, that meteorite craters are produced by explosion of the meteorite. The concept of explosion of the meteorite or of rock heated by impact goes back at least to Merrill (1908, pp. 494–495) and has been elaborated by Ives (1919), Gifford (1924, 1930) and Moulton (1931), followed by many authors in the ensuing decades, notably Baldwin (1949) and Gilvarry and Hill (1956). So widely has this concept been described that craters of inferred high-velocity impact origin are now commonly referred to as explosion craters. In the form developed by Ives and Gifford, the concept of explosion of the meteorite was derived by computing the specific kinetic energy of meteorites travelling in the known range of geocentric velocities of meteors and equating this kinetic energy to specific internal energy in the meteorite at the moment of impact. The specific internal energy was thus found to exceed the enthalpy of vaporization for any solid at atmospheric pressure, and it was concluded that the meteorite would explode.

The error in such a calculation lies in the neglect of the partition of energy in the shock waves generated by the impact and in neglect of the equations of state of the shocked materials. Very high specific energies are produced by hypervelocity impact, but these are the consequence rather than the cause of the shocks which produce the craters. In fact, the fraction of the energy which is retained thermally by material engulfed by shock is unavailable for further propagation of the shock. For the same total energy, the higher the initial specific energy the smaller will be the crater. Vaporization of the meteorite or target rocks would not, therefore, facilitate the opening up of an impact crater, except possibly where the rocks are especially rich in volatile constituents. We may properly speak of meteorite impact craters as explosion craters in the sense that materials fly out of the craters. But in this sense the pits formed by raindrops on soft mud are also explosion craters. It would be better if the term "explosion" were dropped with reference to hypervelocity impact mechanics.

D. Mechanics of Large Meteorite Impact in Rock

When a meteorite strikes the ground at speeds greater than a few km/sec, two shocks are propagated away from the impact interface; one shock advances into the ground and the other shock races back into the meteorite.† The material between the shocks is compressed and its velocity is changed as it is engulfed by the shock fronts. In the general case, where the shape of the meteorite is irregular and the surface of the ground is irregular, the conditions and motion of material between the shocks immediately following impingement are extremely complex. We will touch briefly on some of these complexities later.

The net effect as the shocks advance into the ground and back into the meteorite will be that most of the ground engulfed by shock is accelerated down and outward away from the oncoming body and most of the meteorite engulfed by shock is decelerated and flows in directions paralleling the flow of the underlying shocked rock. Part of the kinetic energy of the meteorite engulfed by shock is converted to internal energy in the meteorite, and part is transferred as kinetic and internal energy to the shocked rock ahead of the meteorite.

A precise calculation of the motion and energy changes of the shocked material would depend upon specifying the shape of the meteorite and target and, for all except the simplest shapes, is beyond present mathematical analysis. A solution in closed form, however, may be readily obtained for the one dimensional case of a semi-infinite meteorite striking a semi-infinite target along a plane interface and in a direction perpendicular to the interface; in addition, Bjork (1958) has obtained a number of specific solutions for the impact along a plane interface of a right circular cylinder of steel into a semi-infinite steel target by numerical integration of the hydrodynamic equations.

It is helpful to examine results for the one dimensional case in order to visualize the conditions of the shocked material and the way in which the energy is partitioned. In this case the two shock fronts are infinite plane surfaces and the material between them has a uniform pressure and velocity. This pressure and velocity and the velocities of the two shocks are each simple functions of the initial velocity of the meteorite, the initial densities of the meteorite and target, and the compression by shock of the meteorite and target. A set of numerical solutions has been obtained for the meteorite and rocks at Meteor Crater, Arizona, for impact velocities of 10, 15, and 20 km/sec by treating the target rocks as a homogeneous system, employing the

† It is not necessary that the speed of the impacting body exceed the acoustic velocity in the target or the meteorite in order to produce a shock.

experimental equation of state for iron, and estimating an average equation of state for the rocks (Shoemaker, 1960*a*, p. 429).

For purposes of illustration, the solutions for only one impact velocity need be examined. Consider the meteorite an infinite plate of iron of thickness T striking the ground at 15 km/sec, the approximate median velocity at which meteorites enter the Earth's atmosphere (Whipple and Hughes, 1955). The pressure between the shocks will be 4·5 Mb and at this pressure the rocks will be compressed 58% and the meteorite will be compressed 43%. At the moment the shock into the meteorite reaches the back side of the plate, the shock into the ground is moving at a speed of 17·2 km/sec and will have advanced a distance of 1·48 T from the original ground surface; the leading face of the meteorite will have penetrated a distance of 0·87 T below the original ground surface and the back side a distance of 0·30 T; the centre of gravity of the compressed system will be 0·78 T beneath the original ground surface and the whole compressed system of rock and meteorite will have a velocity of 10·0 km/sec into the ground. This is the moment of greatest compression of the meteorite. The kinetic energy of the whole compressed system will be $\frac{2}{3}$ and the internal energy $\frac{1}{3}$ of the original kinetic energy of the meteorite. About $\frac{2}{3}$ of the internal energy will be in the compressed rock and $\frac{1}{3}$ in the compressed meteorite and about 53% of the total energy will have been transferred from the meteorite to the compressed rock.

When the shock hits the back side of the plate a tensional or rarefaction wave will be reflected back into the meteorite. The velocity of the meteorite behind the rarefaction will still be about 5·1 km/sec *into the ground*. At the moment the rarefaction reaches the leading face of the meteorite, the shock into the ground will have penetrated about 3·0 T into the ground; the leading face of the meteorite will have penetrated 1·8 T and the back side about 0·8 T beneath the original surface of the ground. The centre of gravity of the moving system will be 1·8 T underground. About 88% of the original kinetic energy of the meteorite will have been transferred to the compressed rock ahead of the meteorite, where the energy will be equally divided into an internal and a kinetic fraction. The compressed rock will still be moving into the ground at 10·0 km/sec.

A meteorite differs importantly from an infinite plate, but these numerical results establish several major qualitative facts about hypervelocity impact. First they show that, by compression alone, an iron meteorite at typical geocentric velocities would penetrate in its entirety below the surface of a target composed of ordinary silicate rocks. Secondly, they show that, even after reflection of a rarefaction from

the back side, the meteorite will not necessarily fly apart but that the whole meteorite may continue to move into the ground. Third, it may be seen that the major part of the original energy of the meteorite is transferred to the shocked rock ahead of the meteorite at a very early stage of penetration. And finally, for the velocity and conditions illustrated, the internal energy of the meteorite never exceeds $\frac{1}{7}$ of the original kinetic energy, and only a fraction of this internal energy will be trapped thermally. A major part of this internal energy is released by expansion of the meteorite behind the rarefaction and contributes to further propagation of the shock into the rock.

The data of Altshuler and others (1958) on the equation of state of iron make it possible to calculate the minimum impact velocity at which the meteorite would have been largely fused by shock at Meteor Crater, Arizona. This velocity was found to be 9·4 km/sec (Shoemaker, in press). From the fact that much of the meteorite now appears to be dispersed as minute spherical drops in fragments of sintered dolomite in the breccia under the crater it was concluded that the impact velocity was greater than 9·4 km/sec. No evidence has been recognized, however, by which it could be shown that more than a small fraction of the meteorite or rocks at Meteor Crater ever behaved as vapour.

In the case of a real meteorite, rarefaction waves are reflected from the sides, which permit lateral flow of the body to take place as well as longitudinal compression. This accentuates the flattening of the body as it penetrates the ground and introduces an additional mechanism of penetration. A rarefaction wave is also reflected from the free surface of the ground, which permits lateral flow of part of the rock engulfed by shock. Material overtaken by the rarefaction waves is deflected laterally from the path of penetration of the meteorite. Both rock and meteorite are swept aside and the meteorite becomes the liner of a transient cavity with material from the rear part of the meteorite facing the centre of the cavity. The additional penetration brought about by lateral flow may be roughly estimated from elementary theory of incompressible fluids. This kind of approximation has been justified on the basis that the pressures greatly exceed the yield strengths of the materials.

In order to compare impact craters with nuclear explosion craters it is necessary to estimate the distribution of shock energy in the walls of the initial cavity formed by the combination of compression and lateral flow of the meteorite and target rocks. This distribution can be expressed as a central point about which the total moment of the energy vanishes. In a homogeneous medium, such a point will be close to the centre of curvature of the shock front after the shock has

propagated some distance from the cavity. This point will be referred to as the apparent centre or apparent origin of the shock. For 15 km/sec impact velocity, the apparent origin of the shock at Meteor Crater, Arizona, was calculated to lie between 4 to 5 diameters of the meteorite beneath the surface, measured along the path of penetration (Shoemaker, 1960*a*, p. 430). The structural evidence appears to require a vertical depth of about this magnitude for the apparent shock origin.

At a more advanced stage in the opening up of the crater the shock and pattern of flow produced by impact begin to resemble more and more closely the shock and flow produced by shallow nuclear explosions. The shock propagates away from the immediate vicinity of the cavity and is followed by the rarefaction reflected from the free surface of the ground. Material engulfed by the shock is accelerated in the directions of shock propagation, which at some distance from the cavity will be approximately along the radii of a sphere. Momentum is trapped in part of the material above the rarefaction wave and it will move upward and outward, individual fragments following ballistic trajectories. As the shock engulfs an ever-increasing volume of rock the shock strength will decrease until ultimately the shock decays to an ordinary elastic wave. The margin of the crater is determined primarily by the radial distance, at the surface, at which there is just sufficient kinetic energy in the rocks behind the reflected tensional wave for fragments to be torn loose and lofted over the rim.

The detailed mechanics of the tearing loose and ejection of pieces at the rim depend on the size of the crater and the depth of initial penetration of the meteorite. In small experimental impact craters in rock, tensile spalling roughly parallel with the rarefaction front appears to determine the shape and size of the crater; in craters the size of the Ries basin and larger, the energy required to actually heave the rocks out is the main factor that determines the size and shape of the crater. For craters of intermediate size, the structure of the rim is sensitive to the depth of the origin of the shock. At Meteor Crater, Arizona, and at the Teapot Ess nuclear explosion crater, where the scaled depth of explosion was comparatively great, the craters were formed mainly by ejection of debris. Beds are sheared off along a roughly conical surface, and the upturning of the strata in the walls of these craters can be looked upon as essentially drag along this shear surface. At the main Odessa crater and the Jangle U crater, on the other hand, where the scaled depth of the explosion was much less, outward flow and buckling in the rim was an important process in the opening up of the craters.

Outward motion of material behind the shock front, as it moves

away from the cavity produced by initial penetration, is not uniform; the pressure soon drops to levels where the strength of the rocks influences the flow. Owing to divergence of the flow, the rocks stretch normal to the flow and break up by tensile fracturing. Meteoritic material and strongly shocked rock are shot out and dispersed in a large volume of broken rock that is relatively only weakly shocked, thus forming a breccia of mixed fragments. Empirically the distance from the origin or centre of the shock to the limit of the mixed breccia in explosion craters is proportional to the cube root of the total shock energy (Shoemaker, 1960*b*). A lens of mixed breccia, roughly proportional in depth to the radius of the crater, may be expected under every large impact crater.

The final phase of displacement of material in fairly large impact craters is the slumping back of the breccia and part of the crater walls toward the centre of the crater. At Meteor Crater, Arizona, this displacement appears to have preceded the showering down of ejecta thrown to great height, but at the Ries basin it may have occurred later. The centripetal movement of material from the crater walls produces a rise in the level of the central part of the crater floor. No sharply defined central hump is present on the floor of Meteor Crater, though a subdued off-centre ridge may be buried under the Pleistocene lake beds below what Barringer (1910; 1924, p. 11) referred to as Silica Hill. The convergent movement resulting from slumping, however, would appear to be entirely adequate to explain the formation of a central hill such as observed in the Steinheim basin.

E. Comparison of Maars and Meteorite Impact Craters

The distinguishing features of maars and large meteorite impact craters are as follows:

(1) Both types of craters have the same gross shape and overlap in range of size. Both are primarily an excavation in the pre-existing terrain encompassed by a rim which is a constructional feature. The relative height of the rim of a maar may vary widely; in principle, the relative height of the rim of impact craters should vary within narrower limits but also varies widely. On Earth true maars are no larger than about 5 km in diameter, though much larger craters of volcanic origin are well known. (All of the larger volcanic craters, referred to as calderas, are believed to have been formed mainly by subsidence, and most are summit features of very large stratovolcanoes.) In contrast, there is no limit, in principle, to the size of impact craters and at least one terrestrial feature of possible impact origin, the Vredefort dome, is much larger than any known volcanic crater.

(2) Both types of craters tend to be approximately circular in plan but may be elliptical or may have polygonal outlines controlled by pre-existing structure. The merging of two or more vents produces compound maar-type craters of irregular outline and, in crater chains, some individual craters are elongated in the direction of the chain. Except for clusters of small craters, impact craters are typically solitary and regular in outline, but in the clusters compound craters have also been found.

(3) Both maars and impact craters may have a central hill or hills, though terrestrial examples are rare.

(4) A maar is underlain by a funnel-shaped volcanic vent filled with a variable assemblage of volcanic tuff and breccia, rocks derived from the vent walls, sediments, and intrusive igneous rocks—in short, a diatreme. An impact crater is underlain by a lens of breccia or crushed, mixed rock. Rocks sintered by shock may be expected to be a universal constituent of such a breccia in large terrestrial impact craters but rarely will constitute more than a few per cent of the breccia.

(5) The country rock is cleanly truncated in the walls of a maar. Except for normal faults, the rocks are rarely deformed in any way that can be related to the opening of the crater. The rocks in the walls of an impact crater, on the other hand, are invariably deformed. Depending on the size, the depth of penetration of the meteorite, and the original structure, beds in the walls may be turned up and overturned, buckled in concentric folds, or sheared out in a series of thrust slices.

(6) Slumping or concentric normal faulting along the crater walls is a common or expectable feature of both maars and large impact craters. The faulting may produce a series of steplike terraces in the crater walls.

(7) The ejecta deposited on the rim of a maar consist both of pieces from the walls of the vent and of new volcanic material, though the new volcanic component may be sparse. Commonly wall rock fragments are present which have come from great depth beneath the crater. Fragments from all sources are generally mixed and scattered through the deposit. Fragments in excess of 3 m in diameter are extremely rare; typical median grain sizes are of the order of 1 cm or less. The ejecta are commonly thinly bedded and, in places, cross bedded.

The ejecta on the rim of an impact crater, on the other hand, except for a minor increment of meteoritic material, are composed solely of rocks excavated from the space occupied by the original crater and the underlying breccia. The fragments are generally stacked approximately in inverted order from their original position before ejection. Thus if the target rocks are initially stratified the ejecta tend to have a mirror stratification. There is no limit to the size of the individual

fragments—the larger the crater the larger are the biggest pieces thrown out. An impact crater the size of an ordinary maar may have on the rim blocks more than 30 m across.

(8) The outer slopes of the rim of a maar are typically smooth. Local relief that may be present is due chiefly to irregularities in the pre-existing topography. The outer slopes of the rim of an impact crater, however, are characteristically hummocky. This is one of the most important criteria that can be used at the present time for identification of impact craters on the Moon.

V. Ballistics of Copernicus

Very few of the features useful in distinguishing an impact crater from a solitary maar on the Moon can be seen under the present limitations of telescopic observation. Much discussion on the origin of lunar craters has centred around statistics of size, shape, and distribution of the craters. By their very nature the statistical arguments are inconclusive and do not lead to the determination of the origin of a single crater. The evidence which has been adduced for the impact origin of lunar craters is thus insufficient.

Many lunar craters are larger than terrestrial maars and all the major lunar craters are larger than any known volcanic crater. But Wright (1927, p. 452) has pointed out that the low gravitational potential on the Moon would result in a far wider distribution of volcanic ejecta on the Moon than on the Earth. For the same magma, boiling would also begin at much greater depth on the Moon. These factors might favour the development of larger craters of the maar type on the Moon than on the Earth, though the size of the chain craters suggests that the influence of these factors is not great.

Baldwin (1949) has shown that the distribution of the depth as a function of the diameter of lunar craters is scattered around a curve extrapolated from data on craters produced by detonation of high explosives. The pertinence of this extrapolation is, at best, not clear. The shape and characteristics of a given crater are sensitive to the scaled depth of the charge or to the penetration of the meteorite. Most of the data on the depths of the lunar craters are old visual measurements of Beer and Mädler (1837) and Schmidt (1878), some of which have large errors. The depth–diameter ratios of lunar craters show about the same broad scatter as ratios for terrestrial volcanic craters, as has been pointed out by Green and Poldervaart (1960, pp. 17–18). In the final analysis we should not expect an especially close relation between the depth–diameter ratios of craters produced by high explosives and impact craters. Because a large amount of gas is

produced, the crater mechanics of high-explosive detonation are substantially different from the crater mechanics of high-velocity impact.

There is one major feature of lunar craters observable from the Earth, however, that may permit unambiguous discrimination of

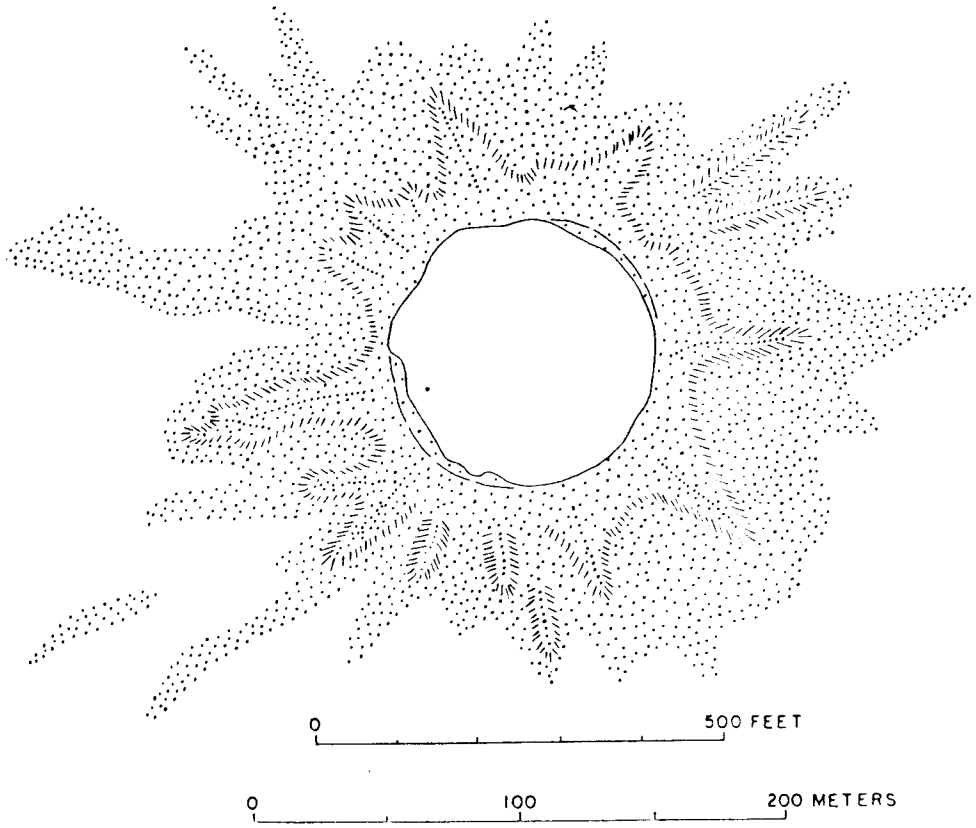

FIG. 9. Ejection pattern at Teapot Ess nuclear explosion crater.

impact craters from volcanic craters. This feature is the distribution pattern of the ejecta. The ejecta from maars are almost invariably thrown out along high-angle trajectories and shower down in a diffuse, more or less uniform, pattern around the crater. These trajectories are the result of entrainment of the fragments in the volcanic gas jets, which are predominantly vertical. The ejecta from large impact craters, on the other hand, are thrown out along both high and low trajectories.

The ejecta pattern around all known large terrestrial impact craters, beyond the immediate vicinity of the rim, has been destroyed by erosion. The general nature of the ejecta pattern to be expected, however, is revealed by the debris deposited around nuclear explosion

craters. Far flung ejecta from nearly every shallow underground explosion crater, whether the explosion is nuclear or chemical, are laid down in distinct streaks or rays (Fig. 9). The position and shape of the rays are governed, in turn, by the pattern in which the ground breaks up as it is engulfed by shock. From the ray pattern and the trajectories of the fragments that form the rays (the exterior ballistics) it is possible to reconstruct the fragmentation pattern of the ground (the interior ballistics of crater formation).

A. Ray Pattern of Copernicus

Many craters on the Moon are surrounded by a system of rays resembling the ejecta patterns around nuclear and high-explosive craters. The ray pattern of Copernicus is especially suited for detailed analysis. Copernicus is favourably located near the centre of the lunar disk; the ray system surrounding the crater is not only widespread but also extends in large part over dark, relatively smooth maria surfaces. Many of the fine details of the system can, therefore, be deciphered (Fig. 4).

The crater itself is somewhat polygonal in outline. It is about 90 km across, and about 3500 m deep, measured from rim crest to floor. The rim rises about 1000 m above the surrounding lunar surface. The interior walls of the crater comprise a series of terraces, scarps, and irregular sloping surfaces that descend stepwise from the crest to the crater floor, a roughly circular area of generally low relief 50 km in diameter. A few low peaks rise above the floor near the centre of the crater.

The outer slopes of the rim are a scaled up version of the outer slopes of the rims of the Jangle U and Teapot Ess nuclear explosion craters. To a lesser extent the rim of Copernicus resembles the rim of Meteor Crater, Arizona. Rounded hills and ridges are combined in a distinctive hummocky array that consists of humps and swales without obvious alignment near the crest of the rim and passes gradually outward into a system of elongate ridges and depressions with a vague radial alignment. The relief of the ridges gradually diminishes until it is no longer discernible at a distance of about 80 km from the crest of the rim. Beyond this distance the rim passes gradationally into the ray system.

The ray system, which extends over 500 km from Copernicus, consists mainly of arcuate and loop-shaped streaks of highly reflective material on a generally dark part of the Moon's surface. In reflectivity characteristics, the rays are essentially an extension of the crater rim and cannot be sharply delimited from it. The major arcs and loops can be locally resolved into en echelon feather-shaped elements, ranging

from 15 to 50 km in length, with the long axes of the elements approximately radially arranged with respect to the centre of the crater.

The pattern of the ray system roughly resembles the pattern of lines of force in a dipole magnetic field in a plane containing the dipole. The "dipole" axis of the Copernican rays trends northwest-southeast. Major arcuate rays curve away from the axis on either side, and a large closed elliptical loop extends southwest toward Mösting.† The ray system has a rough bilateral symmetry about a line coincident with the long axis of this loop, which is perpendicular to the "dipole" axis. Within the main loop extending toward Mösting are subsidiary loops. North of Copernicus are two so-called cross-rays. Both cross-rays consist of a series of vaguely defined loops linked end to end. Near or along the "dipole" axis the rays are mainly straight and radially arranged with respect to Copernicus; in some places, only individual feather-shaped ray elements are present.

Within the rays, and preponderantly near the concave or proximal margins of the major arcs and loops, are numerous elongate depressions or gouges in the lunar surface ranging in length from the limit of telescopic resolution to about 8 km. A peculiar feature of the gouges is their alignment, which is radial from Copernicus in some places but is commonly at an angle to the radial direction. The alignment varies erratically from one gouge to the next. Visible depressions or gouges lie at the proximal ends of many ray elements, though there is not a 1:1 correspondence between gouges and distinguishable ray elements.

It is commonly stated in the literature that there is no determinable relief of the lunar surface associated with the rays. This is not strictly true. At very low angles of illumination the Moon's surface along the rays can be seen to be rough (see Kuiper, 1959*a*, pp. 289–291). The roughness is due, at least in part, to the presence of the gouges and very low rims around the gouges.

The interpretation is here adopted that lunar rays are thin layers of ejecta from the crater about which they are distributed. This interpretation dates back at least to the 19th century and is probably older. The gouges are interpreted as secondary impact craters formed by individual large fragments or clusters of large fragments ejected from Copernicus. Distinct ray elements are interpreted as splashes of crushed rock derived chiefly from the impact of individual large fragments or clusters of fragments. Partial verification of these interpretations is obtained if a full explanation of the ray pattern and associated gouges can be given in terms of the required ballistics.

† The astronomical convention for east and west on the Moon is opposite to the convention used for the Earth.

In order to reduce the ballistic problem of the Copernican rays to a series of discrete points that can be treated mathematically a compilation has been made of 975 secondary impact craters (Fig. 4). This is a conservative compilation and far from complete. The problem of compilation lies in finding the craters, many of which barely exceed the lower limit of resolution on good lunar photographs, and also in distinguishing secondary impact craters belonging to the ray system of Copernicus from other craters of about the same size that are common in this region. Three criteria were used to identify secondary impact craters, and no craters are included in the compilation that did not satisfy at least two of the criteria: (1) markedly elongated shape, (2) shallow depth compared to most small craters outside of ray system, (3) absence of visible rim or extremely low rim. Most small craters in the region around Copernicus that fit these criteria occur in well-defined rays or ray elements, and nearly all such craters that do not lie in the Copernican rays appear to belong to another system of secondary impact craters around the major crater Eratosthenes. The identification of the secondary impact craters is based mainly on one photograph taken by F. G. Pease at the Mount Wilson Observatory, though other photographs from Mount Wilson and Lick Observatories were used as a check.

Two deficiencies in particular should be noted in the present compilation. First, there is a gap in the area around Eratosthenes where no secondary impact craters have been plotted. This gap is due, not to the absence of craters, but to difficulty in distinguishing with certainty the secondary impact craters belonging to the Copernican ray system from craters produced by fragments ejected from Eratosthenes. All craters in the area around Eratosthenes have, therefore, been omitted. The second deficiency is a relative incompleteness of the compilation on the east side of Copernicus, as revealed by the much lower areal density of craters in that area. This defect is due to the fact that, in the principal photographs used for the compilation, the terminator lay to the west of Copernicus and the small secondary impact craters can be distinguished with much higher confidence on the side nearest the terminator.

Ranges of all the secondary impact craters plotted on Fig. 4 were measured from the Mount Wilson photographs. The distance measured was from the tip of the centremost peak on the floor of Copernicus, which is almost precisely at the centre of the circular crater floor, to the nearest point on the rim of each secondary impact crater. These measurements are strictly preliminary and have significant systematic proportional errors in certain directions. The purpose in making the

measurements is simply to find the general nature of the fragmentation pattern that controlled the Copernican rays.

The frequency distribution of the secondary impact craters by range shows a sharp node near 100 miles (about 160 km) from the centre of Copernicus (Fig. 10). At greater distances the frequency drops off

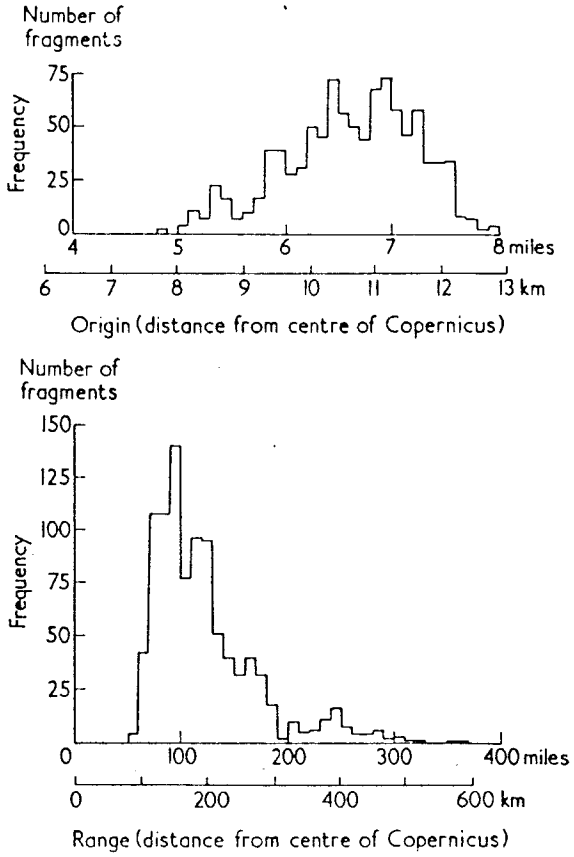

FIG. 10. Frequency distribution of secondary impact crater-forming fragments by range and by calculated original position in Copernicus.

rapidly, but the histogram reveals several subordinate maxima. Toward the outer extremity of the ray system, the frequency drops gradually to zero. Coming closer to Copernicus from the modal distance, the frequency drops off very rapidly, owing to the fact that toward the main crater the gouges in the pre-existing lunar surface tend to be covered up or smothered under an increasingly thick deposit of material making up the crater rim. The smothering effect begins about 80 km from the edge of the crater, and from this point inward there is essentially a continuous blanket of ejecta.

The problem at hand is to deduce the trajectories of the fragments or clusters of fragments that have formed the secondary impact craters

and to solve for the original position of these fragments within the crater. We wish to see if the special pattern of the ray system of Copernicus can be related to a relatively simple pattern of breakup of the rocks within the area of the crater and whether this interior ballistic pattern reflects any of the structural features of the Moon's crust that can be seen in the region around Copernicus. If such a relationship can be found, it will strengthen not only the ballistic interpretation of the rays but also the general features of the crater theory upon which the numerical computations are based.

B. Cratering Theory and Exterior Ballistics

To find the trajectories for individual fragments ejected from Copernicus we require a theory of cratering that gives the relation between ejection velocities and angle of elevation of ejection. A series of approximations and idealization of the cratering problem will be used to obtain a relation in closed form.

First the shock generated by impact will be treated as having an apparent origin at a point some distance below the surface of the ground, corresponding to the centre of gravity of the energy delivered during penetration of the meteorite. This approximation becomes seriously in error within a narrow cone with an axis coincident with the penetration path, but at angles to the probable penetration path that are of interest in explaining the observable features of the Copernican rays the approximation is held to be valid within the limits of variation introduced by inhomogeneities of the surface of the Moon. The exterior ballistics can then be expressed in terms of the geometrical parameters shown on the following diagram, Fig. 11.

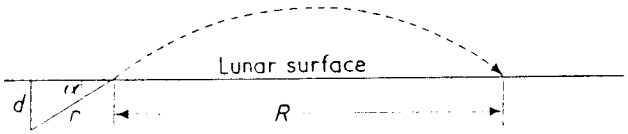

Fig. 11.

d = depth of apparent origin of shock
r = slant radius from apparent origin of shock to surface
α = angle of the slant radius to the horizontal
R = range of trajectory of ejected fragment

From the Rankine-Hugoniot conditions we have the following relations across the shock front:

$$U\rho_0 = (U-\mu)\rho, \qquad \text{(conservation of mass)} \qquad (1)$$

$$P = \rho_0 U\mu, \qquad \text{(conservation of momentum)} \qquad (2)$$

$$e = (1/\rho_0 - 1/\rho)P/2, \qquad \text{(conservation of energy)} \qquad (3)$$

where U is the shock velocity, μ is the particle velocity behind the shock front, ρ_0 is the initial density of the lunar crust, ρ is the density behind the shock front, P is the pressure increment across the shock front, and e is the internal energy increment across the shock front. Combining equations (1), (2), and (3) we have

$$e = (\tfrac{1}{2})\mu^2. \tag{4}$$

Now we shall make an approximation employed successfully by Griggs and Teller (1956, pp. 8–9) to predict shock arrival times in the Jangle U underground explosion in the region of strong shock,

$$E = 2eM, \tag{5}$$

where E is the total shock energy and M is the mass engulfed by shock. This approximation can be derived by assuming that the energy is uniformly distributed in the material behind the shock. Such a distribution is impossible, but the relation gives a fair approximation for the rates of decay of energy, pressure, and shock and particle velocities for shock propagation in rock and leads to a cube root scaling law for the crater diameters. E can be written as

$$E = (\tfrac{1}{2})mv^2, \tag{6}$$

where m is the mass of the meteorite or impacting bolide and v is its velocity. Combining (4), (5), and (6) we have

$$\frac{v^2}{\mu^2} = \frac{2M}{m}. \tag{7}$$

Partly for algebraic simplicity M will be taken as

$$M = (4/3)\pi r^3 \rho_r, \tag{8}$$

where ρ_r is the initial density of the lunar crustal material. This relation preserves cube-root scaling and will minimize the estimate of v. We also may write

$$m = (4/3)\pi x^3 \rho_m, \tag{9}$$

where x is the radius of the bolide, ρ_m its density, and

$$r = \frac{d}{\sin \alpha}. \tag{10}$$

Combining (7), (8), (9), and (10) we have

$$v = \mu \sqrt{\frac{2\rho_r}{\rho_m}} \cdot \frac{1}{\sin^{3/2}\alpha} \left(\frac{d}{x}\right)^{3/2}. \tag{11}$$

For an elastic wave the particle velocity for a point on the surface would be $2\mu \sin \alpha$, but the velocity of a large fragment ejected from a rock surface by shock will be close to μ. This means simply that the kinetic energy imparted by the rarefaction wave reflected from the ground surface is minor, and that the angle of ejection of a fragment from the horizontal lunar surface would be close to α. These relations are consistent with experimental results that have been obtained from large underground explosions.

In order to evaluate equation (11) numerically we must make some assumptions about $\rho_r \rho_m$ and d/x, and an accessory relationship is required relating μ and α. Some minimum requirements of this accessory relationship can be drawn from the ray system of Copernicus.

First, from (4), (5), and (8) we have

$$\mu = \sqrt{\frac{3E}{4\pi\rho_r r^3}}. \tag{12}$$

For a first approximation let us ignore radial variation in the lunar gravitational potential and the departure of the lunar surface from a sphere, and employ the simple classical ballistic formula

$$R = \frac{\mu^2 \sin 2\alpha}{g}, \tag{13}$$

where g is the gravitational acceleration at the surface of the Moon (167 cm/sec^2). We will return to a more precise treatment of the trajectory later. Substituting (10) and (12) into equation (13) we have

$$R = \frac{3E \sin^3\alpha \sin 2\alpha}{4\pi\rho_r d^3 g}, \tag{14}$$

where

$$\frac{3E}{4\pi\rho_r d^3 g} = K \text{ (a constant)}.$$

Now the greatest distance that the Copernican rays can be traced is a little more than 500 km. In order to set a minimum value for v, let us suppose that this distance actually represents the greatest range of fragments. This supposition is demonstrably false, but we will examine it in more detail later. Under this supposition there are two possible trajectories for any range less than the maximum: one for ejection angles higher than the ejection angle for the maximum range, and one for lower ejection angles. For the maximum range we have

$$\frac{dR}{d\alpha} = K(\cos\alpha 4 \sin^3\alpha \cos\alpha - \sin^4\alpha \sin\alpha) = 0, \tag{15}$$

$$\cos \alpha_{max} = \sqrt{1/5}, \quad \alpha_{max} = 63°26'. \tag{16}$$

Substituting the value of α obtained in (16) and $R = 500$ km into equation (13)

$$\mu = \sqrt{\frac{167 \times 5 \times 10^7}{0{\cdot}80}} \text{cm/sec} = 1{\cdot}02 \text{ km/sec}. \tag{17}$$

We are now in a position to evaluate minimum values of v from equation (11). For Meteor Crater, Arizona, a value of d/x of about 8 to 10 was found for $\rho_r/\rho_m = \frac{1}{3}$ and $v = 15$ km/sec (Shoemaker, 1960*a*, p. 430). For the surface of the Moon and likely compositions of the impacting bolide, values of ρ_r/ρ_m between $\frac{1}{2}$ and 1 are more probable. For these higher ratios of the densities lower values of d/x may be anticipated for the same impact velocities. Let us adopt two pairs of values for numerical evaluation (*a*) $\rho_r/\rho_m = \frac{1}{2}$, $d/x = 4$; and (*b*) $\rho_r/\rho_m = 1$, $d/x = 2$. For the velocities that are derived from equation (11), these pairs of values are realistic for the case of Copernicus. Substituting pair (*a*) in (11)

$$(a) \qquad v = \frac{1{\cdot}02 \times 8}{0{\cdot}846} \text{km/sec} = 9{\cdot}6 \text{ km/sec} \tag{18}$$

and

$$(b) \qquad v = \frac{1{\cdot}02 \times 1{\cdot}414 \times 2{\cdot}83}{0{\cdot}846} = 4{\cdot}8 \text{ km/sec}. \tag{19}$$

The interesting fact about these results is that the cratering and ballistic theory presented here leads to the conclusion that the bolide that formed Copernicus was probably an independent member of the solar system, and not a planetesimal or moonlet orbiting around the Earth (cf. Kuiper, 1954, pp. 1108–1111). The value 4·8 km/sec for the impact velocity obtained in (19) is a minimum.

It may be noticed from (14) that the range, as defined, can be made independent of the total energy E and the size of the crater, if the linear dimensions of the shock scale as the cube root of the energy. Thus we would expect practically just as long trajectories from small craters formed by small bolides as from large craters formed by large bolides if the impact velocities are similar. But, in point of fact, there is a rough correlation between size of crater and length of observable rays on the Moon. This can be interpreted to mean that the rays are visible only to the point where the areal density of ejected material is so sparse that it can no longer be photographed or seen, and smaller craters have shorter observable rays because the quantity of ejected

debris is less. When examined closely, it may be seen that the rays die out gradually. There is rarely any suggestion of increase in ray density near the end, such as would be predicted by the maximum range hypothesis. Thus the Copernican rays are formed only by material ejected at low angles and the material ejected at high angles went into escape trajectories.

Employing equation (14) the total range R_T of a fragment from the epicentre of the shock may be written as

$$R_T = K \sin^3\alpha \sin 2\alpha + \frac{d}{\tan\alpha}. \tag{20}$$

From the form of equation (20) it may be seen that the total range, as defined, must pass through a minimum. For a large crater this minimum will be slightly less than the radius of the initial crater produced by ejection of material. At decreasing angles of α, sufficiently low that the total range starts to rise due to rapid increase of the second term, pieces will no longer be thrown out of the crater but will be simply displaced a short distance laterally. A *Schollen- und Schuppen-Zone* or series of thrust sheets may be formed at angles of α where the total range passes through the minimum. In a large crater the final radius of the crater is increased by slumping.

From equation (12) we may write

$$\mu_2^2 = \frac{\sin^3\alpha_2}{\sin^3\alpha_1}\mu_1^2, \tag{21}$$

Thus, if d and any pair of values of μ and α are specified, we may draw a curve for R_T. By successive approximation it may be found that an ejection velocity of 0·4 km/sec for an ejection angle of 12° will lead to the formation of a crater of the lateral dimensions of Copernicus if the centre of gravity of the energy released is at 3·2 km (2 miles) depth. The crater is taken as having been enlarged 25 km by slumping, as measured by the cumulative width of the terraces on the crater walls. From equation (11) the impact velocity is found to be 17 km/sec. At this velocity the centre of gravity of the energy released will be about equal to the linear dimensions of the bolide if the bolide is composed of the same material as the surface of the Moon (calculated from methods given by Shoemaker, 1960*a*). Adopting $d/x = 2$ and a density of 3 for the impacting bolide, the kinetic energy is found to be $7{\cdot}5 \times 10^{28}$ ergs or $1{\cdot}8 \times 10^9$ kilotons TNT equivalent. This may be compared with 1·2 kilotons for the Jangle U experiment; the cube root of the ratio of the energies is $1{\cdot}14 \times 10^3$. As the ratio of the diameters of the two craters is $1{\cdot}1 \times 10^3$, the crater theory employed here gives good

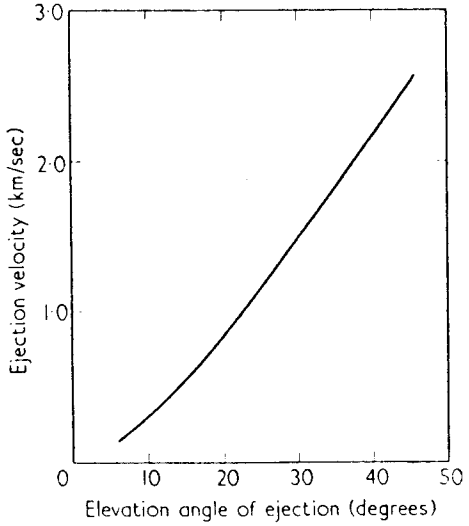

FIG. 12. Ejection velocity as a function of elevation angle of ejection for Copernicus.

agreement with the empirical cube-root scaling law for the diameters of nuclear craters (Glasstone, 1957, p. 198). It should be noted that the scaled depth for the Jangle U shot is slightly greater than that calculated for Copernicus.

The precise equation for the range of the trajectory on a spherical body can be written in the form

$$\phi = \tan^{-1}\frac{\mu^2 \sin\alpha \cos\alpha}{lg - \mu^2 \cos^2\alpha}, \tag{22}$$

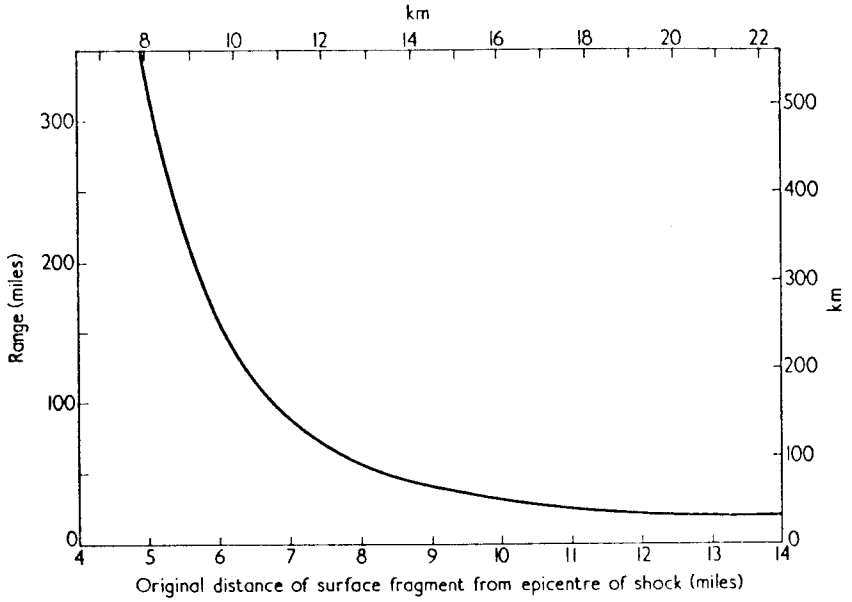

FIG. 13. Range of fragments as a function of original position in crater (Copernicus).

where ϕ is half the angular distance of travel along the surface and l is the radius of the sphere (Giamboni, 1959). For ranges up to 100 km, or about 3° on the lunar surface, the error of equation (13) is small.

Given $\mu = 0{\cdot}4$ km/sec at 12° ejection angle, the ejection velocity may be specified for all ejection angles from equation (20) (see Fig. 12). From equation (22) and the tangent of α, the range of individual fragments initially at the surface may then be expressed as a function of the distance of these fragments from the epicentre of the shock (Fig. 13).

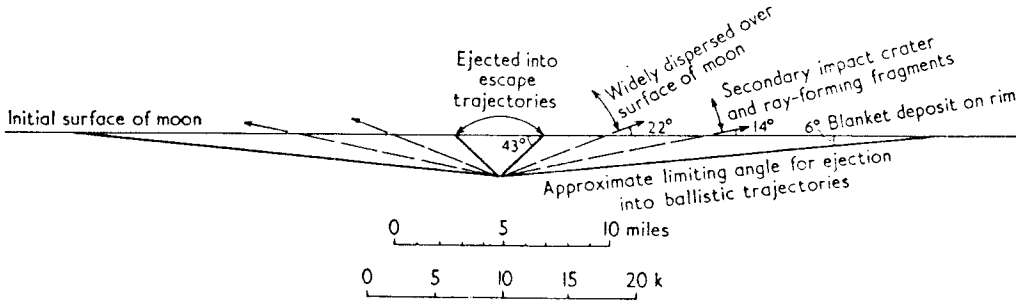

FIG. 14. Provenance of material ejected from Copernicus.

Fragments ejected at angles ranging from about 6° to 14° form the continuous ejecta blanket mantling the rim of Copernicus. The ejected fragments follow a series of overarching trajectories, as required to form the inverted stratigraphy of the rim at Meteor Crater, Arizona. Fragments ejected at angles ranging from about 14° to about 22° form secondary impact craters (the gouges) and the rays (Fig. 14). Between ejection angles of 22° and 43° the smaller volume of material ejected is so widely scattered over the surface of the Moon that it is lost. Above 43° the fragments are ejected into escape trajectories.

C. INTERIOR BALLISTICS

The formation of rays depends upon a departure from the idealized crater model in the real case. Fragments are not ejected precisely along the radii from the apparent shock origin, but are thrown out in distinct clusters or clots. The shape and orientation of these clots as they are first formed in the crater can be found by using the theoretical trajectories to replace the fragments in their approximate original positions.

In order to plot positions within Copernicus for the approximate original loci of the fragments that produced the secondary impact craters, the provisional hypothesis is made that each secondary impact crater was formed by one main fragment and that the fragments all came from a near surface layer. By use of the curve on Fig. 13 all the

fragments are then transposed back into Copernicus along radii from the central point, which is taken as the shock epicentre. In the provisional transposition, the fragments are all found to originate from a circular belt around the shock epicentre (Fig. 15) with an inside radius

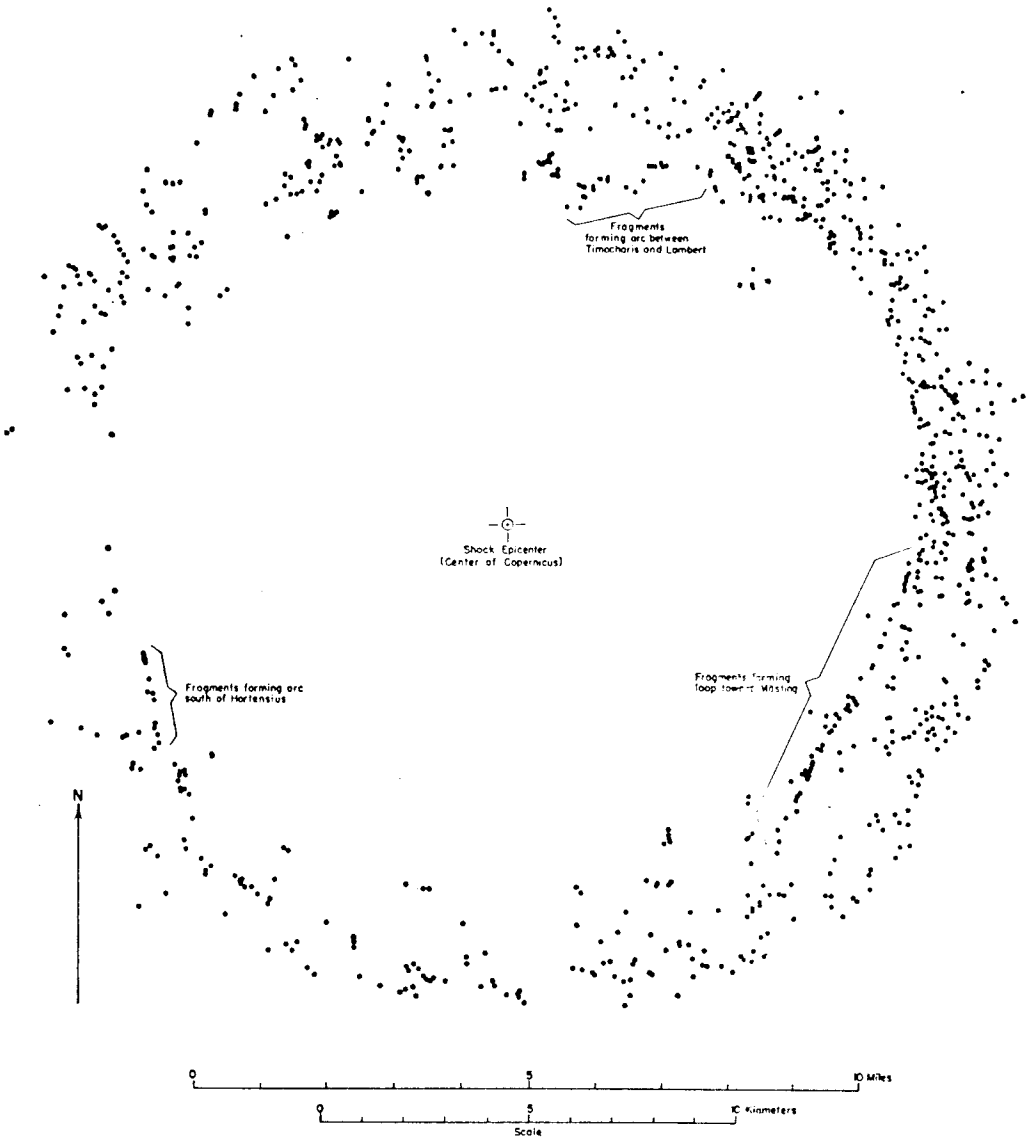

FIG. 15. Provenance of fragments which formed the secondary impact craters in the ray system of Copernicus.

just under 8 km (5 miles) and an outside diameter of 13 km (8 miles). The farthest thrown fragments are derived from the inner margin of the belt.

The large loop-shaped ray extending toward Mösting is found to

have originated from a linear cluster of fragments about 7 km long within Copernicus. The trend of this cluster is essentially parallel with the "dipole" axis of the whole ray system. It is also parallel with a northwest-trending linear system of prominent ridges in the Carpathian Mountains and with the dominant trend of linear topographic features in the general vicinity of Copernicus (Fig. 6). These ridges and linear features are structural elements of the lunar crust that at least in part clearly predate the formation of Copernicus, as will be shown in a later section. The fragmentation pattern thus appears to have been influenced by pre-existing lines of weakness; individual clots of fragments evidently pulled apart along faults and fractures already present in the lunar crust. The linear cluster of fragments that formed the loop-shaped ray toward Mösting is interpreted as a pre-existing structural block that maintained its identity momentarily as it was engulfed by shock. In this way the major features of the ray pattern, the "dipole" axis and axis of symmetry, are controlled by the dominant structural grain of the lunar crust in the vicinity of Copernicus.

Subordinate structural trends also influenced the ray pattern. A prominent arc-like ray that curves around just north of Hortensius is derived from a linear cluster of fragments parallel with a subordinate set of north-northwest trending linear features north of Copernicus and a north-northwest trending set of terraces on the eastern crater wall (Fig. 6). Other linear clusters are also present in the interior ballistic pattern which are parallel with other linear structures in the crater wall and the region around Copernicus.

The significance of these results is that a simple genetic relationship between the main features of the Copernican ray pattern and other observable features of the lunar crust is found by use of the idealized theory of crater formation. The theory accounts quantitatively for both the crater dimensions and the distribution of ejecta. The transposition of rays into linear fragment clusters, however, is not a sensitive test of precision of the computed trajectories. The main features of the interior ballistic pattern would not be significantly changed by minor modification of the relation between the angle of elevation and ejection velocity that was derived from a series of approximations.

We may return now to examine the provisional hypothesis that all the secondary impact crater-forming fragments were derived from a near-surface layer. Material derived from deep positions close to the origin of the shock will be ejected at the same angles as fragments close to the surface. As the near-surface fragments are farthest from the shock origin along any given slant radius and therefore experienced the lowest peak shock pressure, it is reasonable to expect the largest

fragments to have come from near the surface. The question is whether any fragments or clusters of fragments large enough to form secondary impact craters may have originated at significant depth beneath the surface. The frequency distribution of the secondary impact crater-forming fragments and the reconstructed internal ballistic pattern provides some evidence bearing on this question.

The radial frequency distribution of fragments, after transposition into the crater, shows a series of pronounced maxima and minima that correspond to maxima and minima in the original range frequency distribution of the secondary impact craters (Fig. 10). This distribution has been broken down into three sectors around Copernicus (Fig. 16), and the individual maxima may then be identified with major rays or belts of secondary impact craters. In nearly all cases it is found that a maximum in one sector coincides fairly closely in radial position with a maximum in one of the other sectors. Such a coincidence suggests that the interior fragmentation pattern has elements of concentric symmetry around the shock epicentre. A concentric pattern would be found if the lunar crust were layered and clusters of fragments were formed by the separation or pulling apart of layers. This implies that clusters which are separated radially in the fragmentation pattern as plotted on Fig. 15 may actually have been separated vertically in the crater.

Some features of the ray pattern seem easiest to explain by a combination of vertical and horizontal separation of fragment clusters. The very long ray trending north between Timocharis and Lambert, for example, is intersected or joined by two east-west trending cross-rays, one that crosses north of Pytheas, and one that runs just north of Turner. The greatest density of visible secondary impact craters along the north-south ray occurs near the intersections. Such relations could be explained as follows: The north-trending ray was formed by an elongate cluster of fragments with the approximate shape and orientation shown on Fig. 15, but one end of the cluster originally lay at a deeper level than the other in the lunar crust and more than two separable layers were included in the cluster. The uneven distribution of secondary impact craters along the ray would be due to the tendency of the fragments of each layer to hang together momentarily on ejection. This interpretation implies that the fragments of the Turner cross-ray are derived from a different layer than those of the Pytheas cross-ray.

It is not immediately evident which of the two cross-rays, in this interpretation, would represent the deeper layer. Shock propagation theory suggests that, along a given slant radius, the upper layer should have the higher ejection velocity, in which case the Pytheas cross-ray

would represent the higher layer. Empirical evidence from high-explosives cratering experiments, on the other hand, suggests that along certain slant radii fragments from the deeper layer would go farther (Sakharov and others, 1959). The high explosives data may

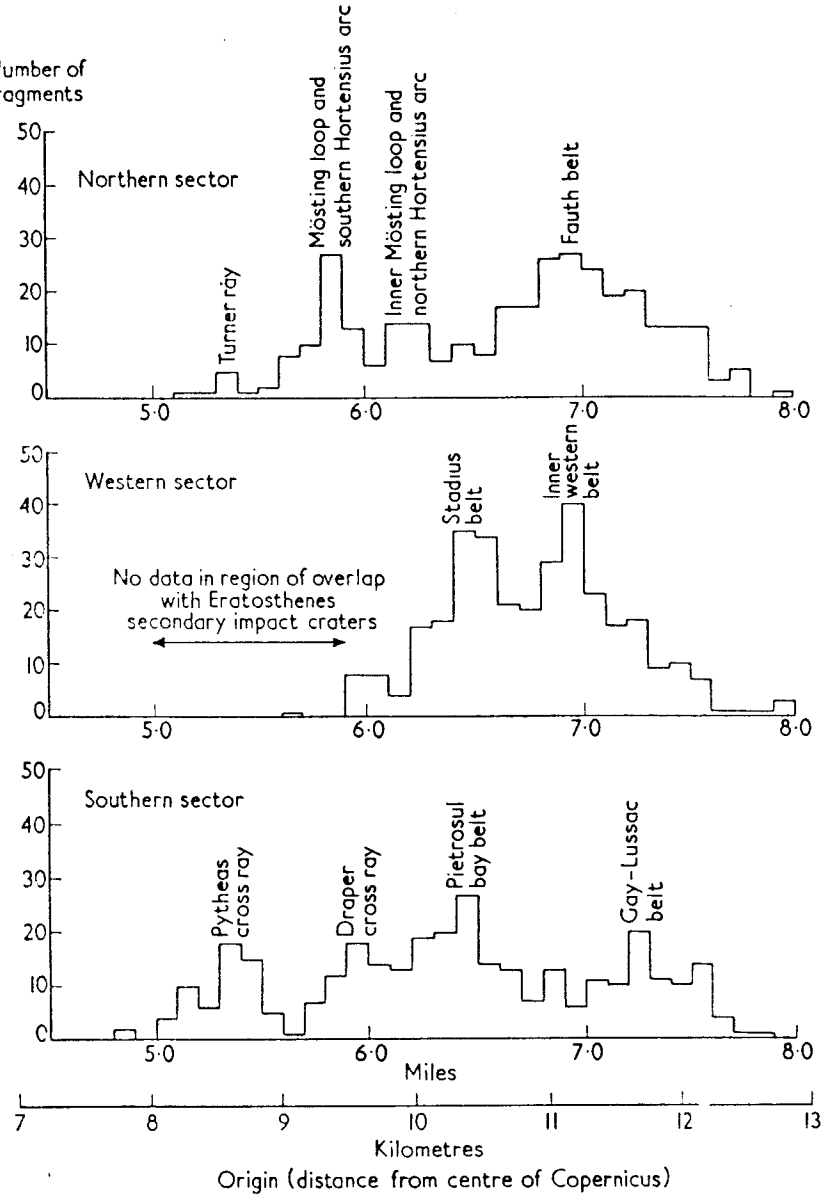

FIG. 16. Frequency distribution (by sectors) of secondary impact crater-forming fragments according to calculated original position in Copernicus.

not be applicable because the fragments are ejected more by the impulse derived from expansion of the explosion gases than by the shock.

Keeping in mind the factors that may influence fragmentation, we may examine the question of the actual size of the fragments that

formed the secondary impact craters. A total of at least 975 fragments are derived from an annular segment of the lunar crust with an area of about 330 km^2, and an unknown depth. If the fragments are assumed to be of equidimensional shape and all derived from one layer, the maximum mean diameter of the fragments would be about 600 m. If the depth from which the large fragments are derived were about three times the mean diameter of the fragments, then the maximum mean diameter would be closer to 1 km. But probably very few, if any, of the fragments that formed the secondary impact craters were as much as a kilometer across. In the first place, a mean diameter of a little less than 1 km would require that essentially all the material ejected at ray-forming angles (Fig. 14) was in large fragments, whereas empirical data on the size frequency distribution of fragments produced by shock shows that about 50% of the material will be in size classes more than an order of magnitude smaller than the maximum size. Secondly, there is a much larger number of secondary impact craters in the visible size range than has actually been compiled. A better guide to the actual size of the fragments is probably provided by the length of cluster of fragments that was ejected towards Mösting to form the loop-shaped ray. At least 50 fragments were derived from a cluster which was only 7 km long. The mean size of the fragments that formed the visible secondary impact craters in the loop-shaped ray was probably in the range of 100 to 200 m in diameter.

These results have an immediate bearing on the origin of the elongate secondary impact craters. Many of the elongate secondary impact craters are oriented at angles to the radial direction from Copernicus and thus cannot be attributed simply to plowing or skidding of the low-angle missile on the lunar surface. Arbitrarily oriented craters could be formed by arbitrarily oriented elongate fragments, but the length required for the fragments is unreasonably great, for some of the secondary impact craters are more than 5 km long. All of the markedly elongate craters are, therefore, probably compound craters formed by the impact of two or more fragments travelling closely together. All gradations can be found, especially along the inner margin of the ray system between short chains of secondary impact craters and compound craters in which the partially merged components can still be recognized. The formation of these chains and compound craters is simply a smaller scale manifestation of the phenomenon of clustering of fragments which is responsible for the broad scale pattern of the rays. Ejection of fragments from large primary impact craters thus provides another mechanism in addition to volcanism by which chains of small craters can be formed on the Moon.

D. Angle of Impact

It is appropriate at this point to return to some questions that were set aside in the discussion of the mechanics of impact and to review the effects of variation of angle of impact, in particular, on the distribution of ejecta.

By ignoring the gravitational attraction of the Moon, Gilbert (1893, pp. 263 and 268) showed that the frequency function dP for the zenith angle of incidence i for bodies approaching from random directions is

$$dP = 2 \sin i \cos i \, di = 2 \sin 2i \, di.$$

The angle of incidence of maximum frequency would therefore be 45°. It may readily be shown that this result is more general, and still applies even when the gravitational attraction of the Moon is taken into account.† In the case of craters formed by the impact of asteroids,

† The case of impact on a massless sphere can be stated as follows. Consider a meteoroid approaching a sphere of radius r from a random direction. Within a circle of the radius of the sphere all points of intersection of the path of the meteoroid with a plane perpendicular to the path are equally probable, and the total probability P is given by

$$P = \pi r^2 = 1.$$

The differential probability or frequency with which the meteoroid will pass through a point at a distance x from the centre of this circle, where $0 \leqslant x \leqslant r$, is

$$dP = 2\pi x dx,$$

and

$$x = r \sin i,$$

where i is the zenith angle of incidence with the sphere (Fig. 17(b)). As

$$dx = r \cos i \, di,$$

then

$$dP = 2\pi r \sin i \, r \cos i \, di = 2\pi r^2 \sin 2i \, di = \sin 2i \, di.$$

In the case of a meteoroid approaching a gravitating body (a homogeneous sphere with mass) from a random direction, the total probability P that the meteoroid intersects a plane perpendicular to the path of the meteoroid within the capture cross-section of radius R is

$$P = \pi R^2 = 1,$$

and the differential probability with which the meteoroid will pass through a point at a distance x from the centre of the capture cross-section, where $0 \leqslant x \leqslant R$, is

$$dP = 2\pi x dx.$$

From conservation of angular momentum we have

$$mxV_\infty = mrV_n,$$

Footnote continued on pp. 342 and 343.

as is indicated for Copernicus by the calculated impact velocity, we will be most frequently concerned with angles of incidence around 45° and instances of vertical incidence have a vanishing probability of occurrence. It should be noticed that very low angles of impact may also be expected to have been of infrequent occurrence.

---

where m is the mass of the meteoroid, V_∞ is the velocity of the meteoroid at infinite distance from the sphere, V_n is the tangential component of the velocity of the meteoroid at the moment of impact and r is the radius of the sphere (Fig. 17(a)). If V_r is the

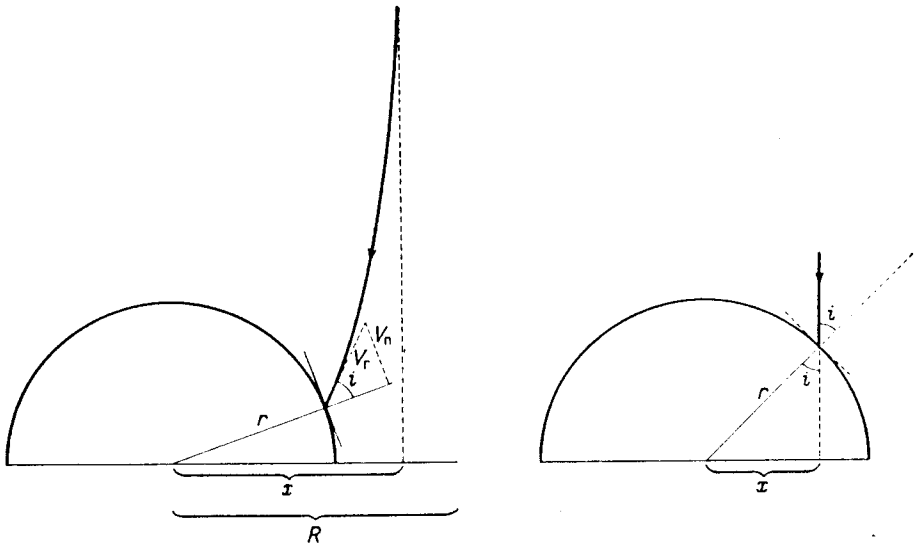

(a) Homogeneous sphere with mass (b) Massless sphere

FIG. 17 (a) and (b). Diagrams illustrating angle of incidence of bodies approaching a sphere from a random direction.

velocity of the meteoroid at the moment of impact and i the zenith angle of incidence,

$$V_n = \sin i \, V_r,$$

$$x = \frac{r V_r \sin i}{V_\infty},$$

$$dx = \frac{r V_r \cos i \, di}{V_\infty},$$

and

$$dP = 2\pi \left(\frac{r V_r \sin i}{V_\infty} \right) \left(\frac{r V_r \cos i \, di}{V_\infty} \right) = \frac{\pi r^2 V_r^2}{V_\infty^2} \sin 2i \, di.$$

But at

$$\sin i = 1, \; x = R,$$

and thus

$$R = \frac{r V_r}{V_\infty}.$$

Small scale hypervelocity experiments show that in the vertical impact of a sphere on a plane surface a small amount of material is ejected, in the beginning stages of penetration, at very flat angles to the surface at velocities exceeding the impact velocity (Charters, 1960). This high speed ejection is evidently due to a jetting effect similar to that produced in the collapse of wedge-shaped liners of shaped charges (Birkhoff *et al.*, 1948). As the penetration proceeds, larger amounts of material are ejected at progressively steeper angles and lower velocities, and in the case of impact into metals the bulk of the material is ejected at angles ranging from about 45° to 65° from the horizontal. This ejection occurs mainly under conditions of hydrodynamic flow; a similar flow regime and mechanics of ejection should prevail for the initial stages of penetration of a large meteorite or asteroid into a rock surface. It is only during the later stages of penetration and cratering that the angle of ejection should decline again as the crater opens up, as indicated in the analysis presented in the preceding pages. At a certain stage of penetration the trend of variation in the angle of ejection is reversed, and there should remain a conical region around the path of penetration, an excluded or forbidden region, through which no fragments may be expected to be ejected.

A pronounced effect on the ray pattern around an impact crater should be found when the zenith angle of incidence is so high that one side of the excluded region becomes parallel or nearly parallel with the Moon's surface. An excluded area for rays would then be expected in the ray pattern around the crater. The ray pattern of Proclus, which has an area with no rays through an arc of about 150° on the southeast side of the crater, is perhaps an example of an ejecta pattern produced by impact at a very high zenith angle. The effect of impact approaching the limiting case of grazing incidence may be illustrated by the highly elliptical crater Pickering, which has just two prominent nearly parallel rays, one extending from each side of the crater in a direction parallel with the long axis of the ellipse. At angles of incidence where the sum of the zenith angle and half the apex angle of the conical excluded region are somewhat less than 90° the ray pattern would probably be asymmetrical, the longest rays extending in the direction

---

Therefore

$$\frac{\pi r^2 V_r^2}{V_\infty^2} = 1,$$

and

$$dP = \sin 2i \, di.$$

in which the impacting body is travelling and the shortest rays in the opposite direction. The ray pattern of Tycho may illustrate this effect.

At the modal angle of impact (45°) the effect of the direction of approach of the bolide on the ray pattern probably becomes negligible. The ejecta most strongly influenced by the asymmetrical flow produced by the oblique penetration are thrown out in escape trajectories. Ray-forming fragments are ejected at greater distances from the path of penetration where the configuration of the shock becomes more nearly symmetrical. The most that can be said from a ray pattern in which the rays extend about equally far in all directions, as in the case of Copernicus, is that the zenith angle of impact was probably not unusually high. Probably the principal effect of increase in the zenith angle of impact is simply to reduce the depth of the apparent origin of the shock.

VI. History of the Copernicus Region

Conclusions as to the origin of Copernicus have wide application, because Copernicus is a member of a large class of lunar craters characterized by a number of distinctive features. The principal feature that unites members of this class is the topography of the rim. The hummocky rim of Copernicus is closely simulated many times over at other craters of similar and smaller size. In general, the ratio of the width of the hummocky terrain to the diameter of the crater decreases with decreasing size of the crater. Around some craters almost all the rim terrain is made up of a nearly random arrangement of hummocks typical of the rim crest at Copernicus; around others the rim is marked by a strong radial or subradial pattern of low ridges typical of the peripheral zone of the rim of Copernicus. Visible gouges or secondary impact craters surround the rims of all such craters approaching Copernicus in size. The interior walls of these craters are almost invariably terraced, the floors are irregular, and nearly all have a central peak or peaks.

Many craters with this group of characteristics are the foci of prominent ray patterns, but many others are entirely unaccompanied by rays. Eratosthenes (Fig. 4) is a good example of a crater that exhibits all the principal topographic features of Copernicus and is surrounded by a well-developed pattern of gouges but lacks rays. Where it is not overlapped by Copernican rays, the rim and floor of Eratosthenes have relatively low reflectivity.

All gradations may be observed in the brightness of the rim and

associated rays of craters of the Copernicus type. Copernicus, Aristillus, and Theophilus illustrate a sequence of craters accompanied by rays ranging from bright to faint. The rays of Aristillus are plainly visible but not as bright as those of Copernicus; the rays of Theophilus are very faint, though its secondary impact craters are widely distributed and as numerous as those of Copernicus. The reflectivity of the rim of Theophilus approaches that of Eratosthenes. It is highly probable that this sequence is one of increasing age of the craters. Wherever a rayless crater of the Copernicus type or a crater with very faint rays occurs in an area with bright rays from some other crater, the bright ray pattern is in all cases superimposed on the darker crater or faint ray pattern; in no instance is a darker ray pattern or rim deposit of a crater of the Copernicus type superimposed on a bright ray. Some process or combination of processes is evidently at work on the lunar surface that causes fading of the rays and other parts of the Moon's surface with high reflectivity. Most of the brightest parts of the Moon's surface are the steepest slopes, where fresh material might be continually exposed by mass movement. Darkening of the surficial materials by radiation damage and mixing of the thin layer of ray material with underlying dark material by micrometeorite bombardment are processes that might well contribute to ray fading.

It is concluded that all craters that exhibit the general topographic features of Copernicus, particularly the hummocky rim and surrounding gouges, are of impact origin.

Other craters of much larger and much smaller size are probably of impact origin as well. Kuiper (1959*b*, p. 1717) has drawn attention to a class of small craters of conical shape or the shape of a truncated cone which he compares with the South African kimberlite pipes, a comparison first made by Eduard Suess (1909, p. 596; 1895, pp. 46–47). An example of such a crater is Hortensius (Fig. 4). Most of these craters have low or inconspicuous rims. The steep inner walls are generally very bright, and some, but not all, have associated rays. It must be borne in mind that the interior and exterior ballistics of impact craters obey different scaling laws and small impact craters on the Moon may have very low rims owing to the wide distribution of the small amount of material ejected. The similarity of the rim of Copernicus to the rims of the much smaller Arizona Meteor Crater and the nuclear explosion craters is partly fortuitous, and is a consequence of the difference in the gravitational potential at the surface of the Moon and Earth which tends to compensate for the difference in size. The presence of rays around some of the conical craters indicates that most craters in this class are probably of impact origin.

At the other extreme of size, the extent of the continuous ejecta deposit of the rim around a very large impact crater tends to be greater in proportion to the diameter of the crater than in the case of Copernicus. As first pointed out by Gilbert (1893, pp. 275–279) Mare Imbrium is partially encompassed by what appears to be an immense sheet of ejecta that extends over a substantial fraction of the visible surface of the Moon. The topography of this sheet is distinctively hummocky in detail, but it is draped over diverse topographic features, some of great size. Mare Imbrium, the apparent source of this sheet of ejecta, or a part of the Mare, evidently represents the largest crater of impact origin on the Moon.

A. Stratigraphy of the Copernicus Region

In the Copernicus region the surface of the Moon is built up mainly of an overlapping series of deposits of ejecta. These deposits, together with layers of material of probable volcanic origin, constitute a stratigraphic succession from which the relative sequence of events in the history of this region can be determined. The deposits have been grouped into five stratigraphic systems: (1) pre-Imbrian, (2) Imbrian, (3) Procellarian, (4) Eratosthenian, and (5) Copernican, which correspond to five intervals of time (Fig. 6).

The Imbrian system: the stratigraphically lowest and oldest system that is widely exposed in the Copernicus region, is made up mainly of the deposit of ejecta derived from the region of Mare Imbrium. The deposit is characterized by a gently rolling "pimply" and "pock-marked" topography that has a shagreen appearance at certain phases. Locally it exhibits a peculiar dark faintly greenish colouration. It has been deposited on a surface of considerable relief that includes old craters and, in the Carpathian Mountains, a series of linear ridges and valleys. The Imbrian ejecta tends to fill in the old craters and valleys and is probably several thousand feet thick where it fills some of these pre-existing depressions, but it is evidently thin where it is draped across the crests of old crater rims and certain high ridges, as indicated by the relative sharpness of form of these features. Some materials of pre-Imbrian age may be locally exposed in areas indicated on Fig. 6.

Material which underlies the relatively smooth dark floors of the Oceanus Procellarum, Mare Imbrium, and Sinus Aestuum rests stratigraphically on the Imbrian system. This material, together with the domes resembling basaltic shield volcanoes, make up the Procellarian system. In reflectivity, the mare floors are indistinguishable from the

volcano-shaped domes, and the mare material is probably composed chiefly of dark volcanic flows, though, except for the domes, typical volcanic features are not readily visible on the maria.

The rim deposits of rayless craters of the Copernicus type are superimposed upon the Imbrian and Procellarian systems. The most extensive of these deposits in the Copernicus region are associated with the craters Eratosthenes, Reinhold, and Landsberg; the whole group of these deposits is taken as the Eratosthenian system. The material making up the narrow rims of rayless conical and truncated cone-shaped craters of the Hortensius type is also included in the Eratosthenian system. These various craters probably have a wide range in age, but all are post-Imbrian and the rim deposits of most rest on the Procellarian. Nearly all are overlapped by Copernican rays.

The Copernican system includes the rays and ejecta deposits of Copernicus and several smaller ray craters, notably Hortensius and a bright ray crater east of Gambart. Among the stratigraphically highest units in the region are the rim deposits of the dark halo craters, which are superposed on the ejecta and rays of Copernicus. These have also been included in the Copernican system.

B. Correlation of the Lunar and Geologic Time Scales

An approximate idea of the correlation of the lunar stratigraphy and the lunar time scale used here with the geologic time scale may be obtained by comparison of the areal density of impact structures and comparison of rates of impact. The areal density of craters interpreted to be of primary impact origin that are superposed on the Procellarian has been examined by R. J. Hackman of the U.S. Geological Survey. He finds that primary impact craters of Eratosthenian and Copernican age that are large enough to be distinguished on photographs (minimum diameter slightly less than one mile) range in density from about 0·24 per 1000 km^2 in Mare Crisium to about 0·53 per 1000 km^2 in Mare Nubium, and average about 0·45 per 1000 km^2 for all the readily visible mare surfaces. If we suppose the end of Procellarian time to have been very early in Earth–Moon history, say 4·5 billion years ago (Patterson, Tilton, and Inghram, 1955), then the mean rate of impact since that time of objects large enough to form craters that may be distinguished photographically is about 0·1 per 1000 km^2 per billion years. The rate of impact of objects large enough to form craters 3 km in diameter would be about 0·05 per 1000 km^2 per billion years.

This rate may be compared with that calculated from the areal density of known probable impact structures (structures of the Sierra Madera type) of about 0·01 per 1000 km^2 in the central United States,

in an area that is geologically favourable for the recognition of impact structures. Most of these structures probably correspond to craters about 3 km in diameter or larger. The average age of the beds exposed in this area is of the order of 300 million years. The rate of impact of objects large enough to form the known structures of the Sierra Madera type in this area is therefore about 0·04 per 1000 km^2 per billion years. This figure is likely to be a minimum because of incompleteness of detailed geologic information on this region and because of the loss from the geologic record of impact events due to erosion. Account must also be taken of the fact that the rate of impact on the Earth should be higher than on the Moon because of the Earth's greater gravitational attraction. For objects entering the Earth's atmosphere at 15 km/sec, the rate of impact on the Earth would be about 2·2 times greater than on the Moon, if the direction of approach were truly random. Several other corrections must be applied, which will be the subject of a separate paper.

When all the factors and uncertainties are considered, the data appear consistent with the hypothesis that the end of Procellarian time is not far removed from the beginning of geologic time and that the rate of impact has been fairly constant since Procellarian time. This hypothesis is in accord with the concept that the objects which formed the Eratosthenian and Copernican impact craters were asteroids, as suggested by the solution for the impact velocity for the bolide which formed Copernicus. It is also possible that some craters may have been formed by the impact of comets.

If the rate of impact has remained steady since the end of the Procellarian (the beginning of the Eratosthenian) we may estimate the age of Copernicus. There are two recognizable craters of probable primary impact origin superimposed on the crater and ejecta rim of Copernicus, an area of about 50,000 km^2. At a rate of 0·1 craters per 1000 km^2 per billion years, this would correspond to an age of about half a billion years for Copernicus. In terms of the geologic time scale this would place Copernicus approximately in the early Paleozoic. The fading of the rays is apparently a slow process. As the rays of Copernicus are toward the brighter end of the range of brightness, the beginning of Copernican time (the age of the faintest rays) is probably well back in Precambrian. On the basis of the relative number of craters, it appears likely that Eratosthenian time covers somewhat more than half of all lunar history.

C. Structure and Structural History of the Copernicus Region

The structure of the Copernicus region comprises old pre-Imbrium

structures, now buried under Imbrian and later strata, folds in the Procellarian, rills and structures of probable volcanic origin of Procellarian or later age, and structures associated with individual craters of the Copernicus and Hortensius type of Eratosthenian and Copernican age.

Pre-Imbrian structures are reflected by the prominent linear ridge and valley topography of the Carpathian Mountains. This topography is a small part of the extensive pattern of linear features termed Imbrian Sculpture by Gilbert (1893, pp. 275–282), the origin of which has been discussed extensively in recent years (Baldwin, 1949, pp. 201–212; Urey, 1951, pp. 220–228; von Bülow, 1957; Kuiper, 1959*a*, p. 310). Trenches, ridges, and scarps in this pattern tend to be approximately aligned along a series of great circles that intersect in the northern part of the Mare Imbrium. The ridges and troughs of the Carpathians are layered over by rocks of the Imbrian system and plunge beneath the Procellarian along the northern margin of Mare Imbrium. Individual ridges that rise above the level of the surrounding Imbrian ejecta are the prominent features of the Carpathians. It is possible that some displacement has occurred along some of these ridges since the Imbrian system was deposited, but there is no apparent displacement of the Procellarian where it overlaps the ridges and valleys along a series of promontories and bays that constitute the mountain front.

To get the full evidence on the origin of the Imbrian sculpture it is necessary to go far beyond the Copernicus region. Gilbert interpreted the large troughs as furrows, plowed by low-angle ejecta; Suess (1895, pp. 38–39) advanced the explanation that they were fissures or graben. Aside from the fact that the trajectories and strength of the ejecta required for the plowing of such furrows are improbable, offsets in the walls of the troughs and ridges show that they are more likely to be fault scarps. It appears highly probable that the Imbrian sculpture is the topographic expression of a radiating set of normal faults that were formed during dilation of the lunar crust by divergent flow behind the shock front generated by the impact that produced the Imbrian ejecta. The ridges of the Carpathians are thus interpreted as horsts; probably they were scarcely formed before they were partially buried by ejecta.

Other linear structures (which have been plotted by R. J. Hackman) also appear to be buried under the Imbrian and higher strata in the Copernicus region (Fig. 6). They are reflected in the alignment of subdued linear topographic features, most of which are best seen stereoscopically. The tectonic fabric, or pattern of faults and fractures, in the pre-Imbrian of this region is probably complex and the product

of numerous structural events besides the impact which produced Imbrian ejecta.

A significant hiatus in time appears to have intervened between the deposition of the Imbrian ejecta and the formation of the Procellarian system, but the evidence for this again lies largely outside of the Copernicus region. The ejecta of several craters that are superposed on the Imbrian ejecta are overlapped by the Procellarian; one of the best examples is the crater Archimedes which lies on the western margin of Mare Imbrium.

Several structural features occur on the maria, in addition to the volcano-shaped features, which may be related closely in time to the emplacement of the Procellarian. These include braided and en echelon systems of low amplitude anticlines or ridges and low scarps that may be monoclines or flow fronts. These features may be chiefly surficial and related to the fluid dynamics of emplacement of the Procellarian system rather than to any broad pattern of stress that affected all or a major segment of the Moon.

A rill on the southwest side of Stadius and the chain crater-rill system north of Stadius (Fig. 6) may be late Procellarian in age or Eratosthenian. They are overlapped by Copernican ejecta and rays.

The structure of craters of Eratosthenian and Copernican ages shown on Fig. 6 is based partly on the observable topography of the craters and is partly inferred from data on terrestrial impact and explosion craters. Copernicus itself is the best example. The well-defined scarps in the crater wall are taken to be normal faults forming the slip surfaces of great slump blocks. These scarps are distinctly linear and show preferred orientations that are probably controlled by pre-Imbrian structure. The outline of the crater, which is somewhat polygonal, has been controlled by the slump faulting. The floor of the crater is inferred to be underlain by a breccia comparable to the breccia of Sierra Madera or perhaps the central breccia of the Vredefort dome. Its depth, shown in the cross-section, is estimated from an empirical scaling relation determined from breccias formed by chemical and nuclear explosions (Shoemaker, 1960*b*), a scaling relation that fits the dimensions of the breccia at Meteor Crater, Arizona. The central peaks of Copernicus are thought to have been raised up in the centre in response to the centripetal slumping of the crater walls. Large Eratosthenian craters have been interpreted in the same way as Copernicus.

Among the latest structural events in the Copernicus region were the formation of the dark-halo craters, here interpreted as maars. If the correlation that has been presented of the lunar time scale is approximately correct, volcanism appears to have been spread over most of

lunar history, though apparently it has changed in character with time. Because of the spatial association of dark-halo craters with Copernicus and the very similar crater Theophilus, there is a suggestion that the later maar-producing volcanism was triggered by impact.

References

Alter, Dinsmore (1957). The nature of the domes and small craters of the moon. *Publ. Astr. Soc. Pacif.* **69,** No. 408, 245–251.

Al'tshuler, L. V., Krupnikov, K. K., Ledenev, B. N., Zhuchikhin, V. I. and Brazhnik, M. I. (1958). Dynamical compressibility and equation of state for iron under high pressure (in Russian). *Soviet J. Exp. Theor. Phys.* **7,** 606–614; translated from Russian in *J. Exp. Theor. Phys.* **34,** No. 4, 874–885, 1958.

Anderson, E. M. (1951). "The Dynamics of Faulting and Dyke Formation with Application to Britain", 2nd edition, Oliver and Boyd, Edinburgh, 206 pp.

Baldwin, R. B. (1949). "The Face of the Moon", Chicago University Press, Chicago, 239 pp.

Barringer, D. M. (1905). Coon Mountain and its crater. *Proc. Nat. Acad. Sci., Wash.* **57,** 861–886.

Barringer, D. M. (1910). "Meteor Crater (formerly called Coon Mountain or Coon Butte) in Northern Central Arizona". Published by the Author, Philadelphia, Pa., 24 pp.

Barringer, D. M. (1914). Further notes on Meteor Crater, Arizona. *Proc. Nat. Acad. Sci., Wash.* **66,** 556–565.

Barringer, D. M. (1924). Volcanoes—or cosmic shell holes; a discussion of the origin of the craters on the Moon and of other features of her surface. *Sci. Amer.* **131,** No. 1, 10–11, 62–63; No. 2, 102, 142–144.

Beals, C. S. (1958). Fossil meteorite craters, *Sci. Amer.* **199,** No. 1, 32–39.

Beals, C. S., Ferguson, G. M. and Landau, A. (1956). A search for analogies between lunar and terrestrial topography on photographs of the Canadian shield, *Roy. Astr. Soc. J.* **2,** 203–211, 250–261.

Beck, C. W. and La Paz, Lincoln (1951). The Odessa, Texas, siderite (ECN = +1025.318) *Pop. Astr.* **59,** 145–151.

Beer, Wilhelm, and Mädler, J. H. (1837). Der Mond nach seinen kosmischen und individuellen Verhältnissen, oder Allgemeine vergleichende Selenographie. Berlin, Simon Schropp, 412 pp.

Bemmelen, R. W. van (1929). Het Caldera probleem [The caldera problem]. *De Mijningenieur*, No. 4, pp. 8–15.

Bentz, Alfred (1925). Die Entstehung der "Bunter Breccie", das Zentral Próblem in Nördlinger Ries und Steinheimer Becken. *Zbl. Miner.*, Abt. B., pp. 97–104, 141–145.

Bentz, Alfred (1927). Geologische Beobachtungen am westlichen Riesrand. Stuttgart, *Dtsch. Geol. Gesell. Z.* **79,** 405–438.

Birkhoff, Garrett, MacDougal, D. P., Pugh, E. M., and Taylor, Sir Geoffrey (1948). Explosives with lined cavities. *J. Appl. Phys.* **19,** 563–581.

Bjork, R. L. (1958). Effects of a meteoroid impact on steel and aluminium in space. *10th Int. Astronaut. Congr.*, London, 1958; preprint, 24 pp.

Boon, J. D., and Albritton, C. C., Jr. (1937). Meteorite scars in ancient rocks. *Field & Lab.* **5,** No. 2, 53–64.

Boon, J. D., and Albritton, C. C., Jr. (1938). Established and supposed examples of meteoritic craters and structures. *Field & Lab.* **6,** No. 2, 44–56.

Boyd, F. R., and England, J. L. (1960). The quartz-coesite transition. *Geophys. Res. J.* **65,** No. 2, 749–756.

Branco, Wilhelm (1895). Schwabens 125 Vulkan-Embryonen und deren Tufferfüllte Ausbruchsröhren; das grösste Maargebiet der Erde: *Wurttemb. Jhefte,* **50,** 505–997 and **51** (1895), 1–337.

Branco, Wilhelm (1902). Das vulkanische Vorries und seine Beziehung zum vulkanischen Ries bei Nördlingen. Berlin, 1902, Phys.-Math. Kl. *Abh. 1, Preuss. Akad. Wiss.*, 1–132.

Branco, Wilhelm (1915). Die vier Entwicklungas tadiem des Vulkanismus. Berlin, *S. B. Preuss. Akad. Wiss.* 59–76.

Branco, Wilhelm, and Fraas, E. (1905). Das kryptovulcanische Becken von Steimheim. Berlin, 1905, Phys. Math. Kl. *Abh. 1, Preuss. Akad. Wiss.*, 1–64.

Brock, B. B. (1951). The Vredefort Ring. *Proc. Geol. Soc. S. Afr.* **53,** 131–157.

Bucher, W. H. (1936). Cryptovolcanic structures in the United States. 16th Internat. Geol. Cong., United States 1933, Rept. **2,** 1055–1084.

Bülow, Kurd von (1954). Die Urkruste des Mondes und der Erde. *Wiss. Z. Univ. Rostock Vg.* **4,** *Math.-Naturw. Reihe No.* 1.

Bülow, Kurd von (1957). Tektonische Analyse der Mondrinde. *Geologie (Berlin),* **6,** 565–609.

Chao, E. C. T., Shoemaker, E. M., and Madsen, B. M. (1960). First natural occurrence of coesite. *Science,* **132,** No. 3421, 220–222.

Charters, A. C. (1960). High-speed impact. *Sci. Amer.* **203,** No. 4, 128–140.

Cotton, C. A. (1952). "Volcanoes as Landscape Forms", 1st edition, revised, John Wiley and Sons, Inc., New York, 416 pp.

Dahmer, Georg (1911*a*). Ein neuer Versuch zur Deutung der Mondoberfläche auf experimenteller Grundlage. *Geol. Rdsch.* **2,** No. 7, 437–440.

Dahmer, Georg (1911*b*). Die Gebilde der Mondoberfläche. *Neues Jb. Min. Geol. Paläont.* **1,** 89–113.

Dahmer, Georg (1912). Die Entstehung der Kraterfelder des Mondes. *Neues Jb. Min. Geol. Paläont.* **2,** 42–44.

Dahmer, Georg (1938). Zur Dampfstosstheorie des Mondreliefs; Ist das Dampftoss-Experiment bloss ein "Modellversuch"? *Geol. Rdsch.* **29,** No. 1, 72–83.

Dahmer, Georg (1952). Die Dampfstosstheorie zur Deutung der Mondkrater. *Naturw. Rdsch.* **5,** No. 11, 458–461.

Daly, R. A. (1946). Origin of the moon and its topography, *Proc. Amer. Phil. Soc.* **90,** No. 2, 104–119.

Daly, R. A. (1947). Vredefort ring-structure of South Africa. *J. Geol.* **55,** No. 3, Pt. 1, 125–145.

Dana, J. D. (1846). On the volcanoes of the moon, *Amer. J. Sci.* Ser. 2, **2,** 335–353.

Darton, N. H. (1905). The Zuñi Salt Lake, *J. Geol.* **13,** 185–193.

Daubrée, Auguste (1891). Recherches Expérimentales sur le rôle possible des gaz à hautes températures, doués de très fortes pressions et animés d'un mouvement fort rapide dans divers phénomènes géologiques. *Bull. Soc. Géol. France* 3rd Ser., **19,** 313–354.

Davis, W. M. (1926). Biographical memoir of Grove Karl Gilbert, 1843–1918. *Mem. Nat. Acad. Sci.* **21,** 5th Mem., 303 pp.

Dehm, Richard (1932). Geologische Untersuchungen im Ries: Das Gebiet des Blattes Monheim. *Neues Jb. Min. Geol. Paläont.* B.–Bd. **67,** Sect. B, 139–256.

Dietz, R. S. (1946). The meteoritic impact origin of the moon's surface features. *J. Geol.* **54,** No. 6, 359–375.

Dietz, R. S. (1959). Shatter cones in cryptoexplosion structures (meteorite impact?). *J. Geol.* **67,** No. 5, 496–505.

Dietz, R. S. (1960). Meteorite impact suggested by shatter cones in rock. *Science,* **131,** No. 3416, 1781–1784.

Dorn, Paul (1948). Ein Jahrhundert Riesgeologie: Berlin. *Dtsch. Geol. Ges. Z.* **100,** 348–365.

Ebert, H. (1890). Ein Vorlesungversuch aus dem Gebiete der physikalischen Geographie (Bildung der Schlammvulkane und der Mondringgebirge). *Ann. Phys. Chem. Neue Folge* **41,** 351–362.

Einarsson, Trausti (1950). The eruption of Hekla 1947–1948. **IV,** 5; The basic mechanism of volcanic eruptions and the ultimate causes of volcanism. *Rit. Visind. Isl.* (Soc. Sci. Islandica), Reykjavík, 30 pp.

Élie de Beaumont, J.B.A.L.L. (1831). Sur les rapports qui existent entre le relief du sol de l'île de Ceylon et de celui de certaines masses de montagnes qu'on aperçoit sur la surface de la Lune. *Ann. Sci. Nat.* **22,** 88–96.

Élie de Beaumont, J.B.A.L.L. (1843). Comparaison entre les masses montagneuses annulaires de la Terre et de la Lune. *C. R. Acad. Sci., Paris,* **16,** 1032–1035.

Ericsson, John (1886). The lunar surface and its temperature: *Nature, Lond.* **34,** 248–251.

Escher, B. G. (1929). On the formation of Calderas. *Leid. Geol. Meded.* **3,** 183–219.

Escher, B. G. (1930). On the formation of Calderas. *IV Pacif. Sci. Cong., Proc.* **2,** 571–589.

Escher, B. G. (1949). Origin of the asymmetrical shape of the earth's surface and its consequences upon volcanism on earth and moon. *Bull. Amer. Geol. Soc.* **60,** No. 2, 352–362.

Escher, B. G. (1955). Three caldera-shaped accidents; volcanic calderas, meteoric scars and lunar cirques, *Int. Volcan.* Ser. 2, **16,** 55–70.

Fairchild, H. L. (1938). Selenology and cosmogeology; cosmic and geologic import of the lunar features. *Science* n.s., **88,** No. 2294, 555–562.

Faye, H. A. (1881). Les volcans de la lune. *Rev. Sci.* ser. 3, **1,** 130–138.

Firth, C. W. (1930). The Geology of the North-west portion of Manukau County, Auckland. *Trans. Proc. N.Z. Inst.* **61,** 85–137.

Forbes, V. S. (1929). The moon and radioactivity. *Geol. Mag.* **66,** 57–65. Reprinted with additions, 1931, *Smithson. Inst. Ann. Rept.* (1930), 207–217.

Galbraith, F. W. (1959). Craters of the Pinacates: Arizona Geol. Soc., "Southern Arizona Guidebook 2", pp. 161–164.

Gerstlauer, K. (1940). Geologische Untersuchungen im Ries: Das Gebiet des Blattes Offingen: München, *Abh. Geol. Landesuntersuch. Bayer. Oberberg.* **35.**

Giamboni, L. A. (1959). Lunar rays: their formation and age. *Astrophys. J.* **130,** 324–335.

Gifford, A. C. (1924). The mountains of the Moon. *N.Z. J. Sci. Tech.* **7,** 129–142.

Gifford, A. C. (1930). The origin of the surface features of the Moon. *N.Z. J. Sci. Tech.* **11,** 319–327.

Gilbert, G. K. (1893). The moon's face; a study of the origin of its features. *Bull. Phil. Soc. Wash.* **12,** 241–292.

Gilbert, G. K. (1896). The origin of hypotheses, illustrated by the discussion of a topographic problem. *Science*, n.s. **3**, 1–13.

Gilvarry, J. J., and Hill, J. E. (1956). The impact of large meteorites. *Astrophys. J.* **124**, No. 3, 610–622.

Glasstone, Samuel, ed. (1957). "The Effects of Nuclear Weapons". Washington D.C., U.S. Atomic Energy Commission, 579 pp.

Goodacre, Walter (1931). "The Moon, with a Description of Its Surface Formations." Published by the author, Bournemouth, England, 364 pp.

Green, Jack, and Poldervaart, Arie (1960). Lunar defluidization and its implications, XXI Internat. Geol. Cong. Rept. of Sessions, Pt. 21, 15–33.

Griggs, D. T., and Teller, Edward (1956). Deep underground test shots. California Univ. Radiation Lab. Rept. 4659, 9 pp.

Gruithuisen, F. von P. (1829). "Analekten Erd- und Himmels-Kunde", München, 2.

Günther, Siegmund (1911). "Vergleichende Mond- und Erd-kunde". Braunschweig, F. Vieweg und Sohn, 193 pp.

Hack, J. T. (1942). Sedimentation and volcanism in the Hopi Buttes, Arizona: *Bull. Amer. Geol. Soc.* **53**, No. 2, 335–372.

Hall, A. L. and Molengraaff, G.A.F. (1925). The Vredefort Mountain land in the southern Transvaal and the northern Orange Free State. *Verh. Akad. Wet. Amst.* Sect. 2, No. 3, Pt. 24, No. 1–183.

Hannay, J. B. (1892). Formation of lunar volcanoes. *Nature, Lond.* **47**, 7–8.

Hardy, C. T. (1953). Structural dissimilarity of Meteor Crater and Odessa meteorite crater. *Bull. Amer. Ass. Petrol. Geol.* **37**, 2580.

Hardy, C. T. (1954). Major craters attributed to meteoritic impact. *Bull. Amer. Ass. Petrol. Geol.* **38**, No. 5, 917–923.

Herschel, William (1787). An account of three volcanoes in the Moon. *Phil. Trans.* p. 229.

Hooke, Robert (1665). "Micrographia", London, J. Martyn and J. Allestry, 246 pp.

Hopmann, Michael, Frechen, Josef, and Knetsch, Georg (1956). "Die Vulkanische Eifel". Bonn, Wilhelm Stollfuss Verlag, 143 pp.

Hubbert, M. K. (1937). Theory of scale models as applied to the study of geologic structures. *Bull. Amer. Geol. Soc.* **48**, No. 10, 1459–1519.

Hubbert, M. K. and Willis, D. G. (1957). Mechanics of hydraulic fracturing. *Trans. Amer. Inst. Mining Engrs.* **210**, 153–168.

Humbolt, Alexander von (1863). "Cosmos: A Sketch of a Physical Description of the Universe", vol. 4 (translated from German by E. C. Otté and B. H. Paul). New York, Harper and Brothers, 234 pp.

Ives, H. E. (1919). Some large-scale experiments imitating the craters of the moon. *Astrophys. J.* **50**, 245–250.

Jaggar, T. A., Jr. and Finch, R. H. (1924). The explosive eruption of Kilauea in Hawaii. *Amer. J. Sci.* 5th ser., **8**, 353–374.

Jahns, R. H. (1959). Collapse depressions of the Pinacate volcanic field, Sonora, Mexico. Arizona Geol. Soc., "Southern Arizona Guidebook 2", 165–184.

Jeffreys, Harold (1959). "The Earth: its Origin, History and Physical Constitution", 4th edition. Cambridge Univ. Press, 420 pp.

Joesting, H. R. and Plouff, Donald (1958). Geophysical studies of the Upheaval Dome area, San Juan County, Utah, *in* "Guidebook to the Geology of the Paradox Basin." Intermountain Assoc. Petroleum Geologists, 9th Ann. Field Conf., 86–92.

Judd, J. W. (1888). The eruption of Krakatoa and subsequent phenomena. "Report of the Krakatoa Committee of the Royal Society, Pt. I", London, Trübner and Co.

Kant, J. (1785). Die Vulkane im Monde: Leipzig Naturwiss. Schriften von J. Kant, (Insel- Verlag) 1912, 425–433.

Karpoff, Roman (1953). The meteorite crater of Talemzane in southern Algeria. *Meteorites* **1**, 31–38.

King, P. B. (1930). "The geology of the Glass Mountains, Texas. Pt. 1, Descriptive geology". *Texas Univ. Bull.* 3038, 167 pp.

Kranz, Walter (1911). Das Nördlinger Riesproblem: Stuttgart. *Jb. Oberhein. Geol. Ver.* N.F.1, 32–35.

Kranz, Walter (1934). Fünfte Fortsetzung der Beiträge zum Nördlinger Ries-Problem. *Zbl. Miner.* pt. B, No. 6, 262–271.

Krejčí-Graf, Karl (1928) Der Bau des Mondes. *Natur u. Mus. Rep.* 58, No. 8, 337–346; No. 9, 395–405; No. 10, 449–460; No. 11, 510–518.

Krejčí-Graf, Karl (1959). Der Bau der Mondoberfläche im Vergleich mit der Erde Daten und Deutung. *Astronautica Acta*, **5**, Nos. 3–4, 163–223.

Kuiper, G. P. (1954). On the origin of the lunar surface features. *Proc. Nat. Acad. Sci. Wash.* **40**, No. 12, 1096–1112.

Kuiper, G. P. (1959*a*). The exploration of the moon, *in* "Vistas in Astronautics", 2nd Annual Astronaut. Symposium. New York, Pergamon Press, Vol. 2, 273–312.

Kuiper, G. P. (1945*b*). The moon. *J. Geophys. Res.* **64**, 1713–1719.

Lee, W. T. (1907). Afton craters of southern New Mexico. *Bull. Amer. Geol. Soc.* **18**, 211–220.

Leonard, F. C. (1946). Authenticated meteoritic craters of the world, *in* "A Catalog of Provisional Coordinate Numbers for the Meteorite Falls of the World". Albuquerque, New Mexico Univ. Pub. Meteoritics No. 1, New Mexico Univ. Press.

Lord, J. O. (1941). Metal structure in Odessa, Texas, and Canyon Diablo, Arizona, meteorites. *Pop. Astr.* **49**, 493–500.

Marshall, R. K. (1943). Origin of the lunar craters, a summary. *Pop. Astr.* **51**, 415–424.

Matheson, G. L., Herbst, W. A., Holt, P. H. and others (1949). Dynamics of fluid-solid systems. Fifteenth annual chemical engineering symposium; Division of Industrial and Engineering Chemistry, American Chemical Society. *Industr. Engng. Chem.* **41**, No. 6, 1099–1250.

Matoušek, Otakar (1924a). Study in comparative cosmic geology, I. The district of Sinus Iridium on the moon (in Czech, with English summary). *Říše Hvězd* **5**, 1–12.

Matoušek, Otakar (1924b). Studien aus der vergleichenden Kosmischen Geologie; Die Gegend Sinus Iridium am Monde. *Zbl. Miner. Geol. Paläont.* No. 1, 10–17.

Matoušek, Otakar (1930). Tectonics of the moon. *Pan-Amer. Geol.* **54**, No. 2, 81–86.

McKnight, E. T. (1940). Geology of area between Green and Colorado Rivers, Grand and San Juan Counties, Utah *Bull. U.S. Geol. Survey*, 908, 147 pp.

Merrill, G. P. (1908). The meteor crater of Canyon Diablo, Arizona; its history, origin, and associated meteoritic ions. *Smithson. Inst. Misc. Coll.* **50**, 461–498.

Meydenbauer, A. (1877). Über die Bildung der Mondoberfläche. *Sirius Lpz.* **10**, 180.

Meydenbauer, A. (1882). Die Gebilde der Mondoberfläche. *Sirius Lpz.* **15**, 59–64.

Miller, Ephraim (1898). A new theory of the surface markings of the moon. *Trans. Kansas Acad. Sci.* **15**, 10–13.

Mohorovičič, Stepan, (1928). Experimentelle Untersuchugen über die Entstehung der Mondkrater, ein neuer Beitrag zur Explosionshypothese (Croatian with German summary): *Archiv za Hemiju i Farmaciju, Zagreb*, **2**, 66–76.

Moulton, F. R. (1931). "Astronomy". New York, MacMillan Co., 549 pp.

Müller, G. and Veyl, G. (1957). The birth of Nilahue, a new maar type volcano at Riñinahue, Chile. XX Internat. Geol. Cong. Rept., Sect. 1, 375–396.

Nathan, Hans (1925). Geologische Untersuchungun im Ries. Das Gebiet des Blattes Möttingen. *Neues Jb. Miner. Geol. Paläont.* B.-Bd. **53**, B, 31–97.

Nathan, Hans (1935). Geologische Untersuchungen im Ries. Das Gebiet des Blattes Ederheim: München. *Abh. Geol. Landesuntersuch. Bayer. Oberberg.* No. 19, 42 pp.

Nasmyth, J. H. and Carpenter, J. (1885). "The Moon". New York, Scribner and Welford.

Nel, L. T. (1927). The geology of the country around Vredefort; an explanation of the geological map. South Africa Dept. Mines and Industries, Geol. Survey, 134 pp.

Nevill, E. N. (Neison, Edmund, pseudonym) (1876). "The Moon and the Condition and Configurations of its Surface". London, Longmans, Green and Co., 576 pp.

Odé, Hans (1956). A note concerning the mechanism of artificial and natural hydraulic fracture systems. *Colo. Sch. Min. Quart.* **51**, No. 3, 19–29.

Ordoñez, Ezequiel (1905). Los Xalapazlos del Estado de Puebla. *Parerg. Inst. Geol. Mex.* **1**, 295–344.

Ower, L. H. (1929). The moon and radioactivity. *Geol. Mag.* **66**, 192.

Patterson, C. C., Tilton, G. R. and Inghram, M. G. (1955). Age of the earth. *Science*, **121**, 69–75.

Peal, S. E. (1886). Lunar glaciation. *Nature Lond.*, **35**, 100–101.

Pecora, W. T. (1960). Coesite craters and space geology. *Geotimes* **5**, No. 2, 16–19, 32.

Perret, F. A. (1912). The flashing arcs: a volcanic phenomenon. *Amer. J. Sci.* Ser. 4, **34**, 329–333.

Perret, F. A. (1924). The Vesuvius eruption of 1906; study of a volcanic cycle. Carnegie Inst. Wash., Publ. No. 339, 151 pp.

Pickering, W. H. (1903). "The Moon; a Summary of the Existing Knowledge of our Satellite with a Complete Photographic Atlas". New York, Doubleday, Page and Co., 103 pp.

Pickering, W. H. (1906). Lunar and Hawaiian physical features compared. *Mem. Amer. Acad. Arts Sci.* **13**, 149–179.

Proctor, Mary (1928). "Romance of the Moon". New York, Harper & Bros., 262 pp.

Proctor, R. A. (1873). "The Moon, her Motions, Aspect, Scenery and Physical Condition". Manchester, Alfred Brothers, 394 pp. (Second Edition, 1878, London, Longmans, Green and Company, 314 pp.).

Quiring, Heinrich (1946). Gedanken über Alter, Zusammensetzung und Entstehung des Mondes: *Z. Dtsch. Geol. Ges.* **98**, 172–187.

Reck, Hans, ed. (1936). Santorin, der Werdegang eines Inselvulkans und sein Ausbruch 1925–1928. Berlin, Dietrich Reimer, 3 vols.

Reich, Hermann, and Horrix Wilhelm (1955). Geophysikalische Untersuchungen im Ries und Vorries und deren geologische Deutung. Hannover, Beihefte zum *Geol. Jb.* No. 19, 119 pp.

Reiche, Parry (1940). The origin of Kilbourne Hole, New Mexico. *Amer. J. Sci.* **238**, No. 3, 212–225.

Reuter, Lothar (1925). Die Verbreitung jurassischer Kalkblocke aus dem Ries im sudbayr. Diluvialgebiet: *Jber. Mit. Oberrhein. Geol.* N.F. **14**, 191–218.

Rozet, M. le Capitaine (1846). Sur la sélénologie. *C.R. Acad. Sci., Paris*, **22**, 470–474.

Russell, I. C. (1885). Geological history of Lake Lahontan, a Quaternary lake of northwestern Nevada. U.S. Geol. Survey Mon. 11, 288 pp.

Sacco, Federico (1907). "Essai Schématique de Sélénologie". Turin, G. Clausen-H. Rinck suco., 47 pp.

Sacco, Federico (1948). Considérations sur la genèse lunaire. *Bull. Belge. Géol. Pal. Hydr.* **57**, Pt. 2, 240–245.

Sakharov, V. N., Kolesnikov-Svinarev, V.I., Nazarenko, V.A. and Zabidarov, E.I. (1959). Local distribution of earth thrown up by underground explosions. *C.R. Acad. Sci. U.R.S.S.* **124**, 21–22.

Sauer, Adolf (1901). Petrographische Studien an den Lavabrocken aus dem Ries: *Jb. Vaterl. Naturk. Württembg.* **57**.

Schmidt, J. F. J. (1878). "Die Charte der Gebrige des Mondes". Berlin, Dietrich Reimer, 303 pp.

Schröder, Jöachim and Dehm, Richard (1950). Geologische Untersuchungen im Ries. *Abh. Naturw. Ver. Schwaben e. V. in Augsburg*, **5**, 147 pp.

Schwarz, E. H. L. (1909). The probability of large meteorites having fallen upon the earth. *J. Geol.* **17**, 124–135.

Schwarz, E. H. L. (1927). Cauldrons of subsidence. *Geol. Mag.* **56**, 449–457.

Schwarz, E. H. L. (1928). Terrestrial and lunar faults compared. *J. Geol.* **36**, No. 2, 97–112.

Scrope, G. P. (1862). "Volcanoes". London, Longman, Green, Longmans and Robert, 490 pp.

Sellards, E. H., and Evans, G. L. (1941). Statement of progress of investigation at Odessa meteor craters. Texas Univ., Bur. Econ. Geology, 12 pp.

Shaler, N. S. (1903). A comparison of the features of the earth and moon: *Smithson. Contrib. Knowl.* **34**, No. 1438, 1–130.

Shoemaker, E. M. (1956). Occurrence of uranium in diatremes on the Navajo and Hopi reservations, Arizona, New Mexico, and Utah; *in* Page, L. R., Stocking, H. E. and Smith, H. B., Contributions to the geology of uranium and thorium by the United States Geological Survey and Atomic Energy Commission for the United Nations International Conference on Peaceful Uses of Atomic Energy, Geneva, Switzerland 1955; U.S. Geol. Survey Prof. Paper 300, 179–185.

Shoemaker, E. M. (1957). Primary structures of maar rims and their bearing on the origin of Kilbourne Hole and Zuñi Salt Lake, New Mexico (abs.). *Bull Amer. Geol. Soc.* **68**, No. 12, Pt. 2, 1846.

Shoemaker, E. M. (1960*a*). Penetration mechanics of high velocity meteorites, illustrated by Meteor Crater, Arizona. XXI Internat. Geol. Congr. Rept., Pt. 18, 418–434.

Shoemaker, E. M. (1960*b*). Brecciation and mixing of rock by strong shock. *U.S. Geol. Survey Prof. Paper* 400-B, 423–425.

Shoemaker, E. M. (in press). Impact mechanics at Meteor Crater, Arizona, *in* Kuiper, G.P., ed., "The Solar System", Chicago, Chicago Univ. Press, Vol. 4, Pt. 2.

Shoemaker, E. M., Roach, C. H. and Byers, F. M., Jr. (in press). Diatremes and Cenozoic geology of the Hopi Buttes region, Arizona. *Bull Amer. Geol. Soc.*

Shoemaker, E. M., and Chao, E. C. T. (1960). Origin of the Ries basin, Bavaria, Germany (abs.). *Bull. Amer. Geol. Soc.* **71,** 2111–2112.

Simeons, G. (1906). À propos d'une récente tentative de comparaison entre la constitution de la terre et celle de la lune. *Bull. Soc. Belge Geol. Pal. Hydr.* **19,** Proc.-verb. 204–215.

Smith, S. P. (1887). The Eruption of Tarawera. A Report to the Surveyor-General. Wellington, New Zealand Government Printer, 84 pp.

Spencer, L. J. (1933). Meteorite craters as topographical features on the earth's surface. *Geog. J.* **81,** No. 3, 227–248.

Spencer, L. J. (1937). Meteorites and the craters on the moon. *Nature, Lond.* **139,** No. 3520, 655–657.

Spurr, J. E. (1944). "Geology Applied to Selenology": Vol. I "The Imbrian Plain Region of the Moon". The Science Press Printing Co., Lancaster, Pa., 112 pp.

Stearns, H. T. (1925). The explosive phase of Kilauea volcano, Hawaii, in 1924. *Bull. Volcan.* **5/6,** 193–208.

Stearns, H. T. and Vaksvik, K. N. (1935). Geology and ground-water resources of the island of Oahu, Hawaii. Hawaii Terr. Dept. Public Lands Div. *Hydrogr. Bull.* **1,** 479 pp.

Stehn, C. E. (1929). The geology and volcanism of the Krakatau group. IV Pacif. Sci. Congr., Java, 55 pp.

Stutzer, Otto (1936). "Meteor-Crater", Arizona und Nördlinger Ries. *Z. Dtsch. Geol. Ges.* **88,** No. 8, 510–523.

Suess, Eduard (1895). Einige Bemerkungen über den Mond. *S.B. Akad. Wiss. Wien. Math.-Naturwiss Kl.* **104,** Pt. 1, No. 2, 21–54.

Suess, Eduard (1909). "The Face of the Earth", Volume IV (English translation). Oxford, Clarendon Press, 673 pp.

Suess, F. E. (1917). Gestalten der Mondoberfläche. *Geol. Gesell. Wien Mitt.* **10.** 218–248.

Thiersch, August, and Thiersch, H. W. J. (Asterios) (1899). "Die Physiognomie des Mondes". Nördlingen.

Thomas, A. P. W. (1888). Report on the eruption of Tarawera and Rotomahana, New Zealand. Government Printer, Wellington, New Zealand, 74 pp.

Tilghman, B. C. (1905). Coone Butte, Arizona. *Proc. Philad. Acad. Nat. Sci.* **57,** 887–914.

Tomkins, H. G. (1927). The igneous origins of some of the lunar formations. *J. Brit. Astr. Ass.* **37,** No. 5, 161.

Treibs, Walter (1950). Geologische Untersuchungen im Ries; das Gebiet des Blattes Otting. *München Geol. Bavar.* **3,** 52 pp.

Urey, H. C. (1951). The origin and development of the Earth and other terrestrial planets. *Geochim. et Cosmochim. Acta.* **1,** 209–277.

Verbeek, R. D. M. (1886). "Krakatau". Batavia, Imprimerie de l'Etat, 567 pp. and Atlas in 2 volumes.

Viete, Gunter (1952). Geologie und Mondoberfläche. *Die Bergakad. Freiberg*, **4**, No. 12, 470–482.

Wagner, P. A. (1914). The diamond fields of Southern Africa. *The Transvaal Leader*, Johannesburg, Union of South Africa, 347 pp.

Wasiutyński, Jeremi (1946). Studies on hydrodynamics and structure of stars and planets. *Astrophys. Norvegica*, **4**, 497 pp.

Wegener, Alfred (1920). Die Aufsturzhypothese der Mondkrater. *Sirius Lpz.* **53**, 189.

Wegener, Alfred (1921). Die Entstehung der Mondkrater. Braunschweig, Sammlung Vieweg, Tayesfragen. *Natur. u. Tech.* **55**, 48 pp.

Wegener, Alfred (1922). Versuche zur Aufsturztheorie der Mondkrater. *S. Nova Acta Leop. Carol.* **106**, No. 2, 107–118.

Werner, E. (1904). Das Ries in der Schwäb.-fränk. *Blätter Schwäb. Albver.*

Whipple F. L., and Hughes R. F. (1955). On the velocities and orbits of meteors, fireballs and meteorites. *J. Atmos. Terres. Phys.* Suppl. 2, 149–156.

Wilkins, H. P., and Moore, P. A. (1955). "The Moon", London, Faber & Faber Ltd., 388 pp. Also MacMillan and Co. Inc., New York.

Williams, Howel (1941). Calderas and their origin. *Calif. Univ. Bull. Geol. Sci.* **25**, No. 6, 239–346.

Wilson, C. W. (1953). Wilcox deposits in explosion craters, Stewart County, Tennessee, and their relations to origin and age of Wells Creek Basin structure. *Bull. Amer. Geol. Soc.* **64**, No. 7, 753–768.

Wolff, F. L. von (1914). *Der Vulkanismus.* Stuttgart, Ferdinand Enke, Verlag, Allgemeiner Teil, Pt. 2, **1**, 301–711.

Wright, F. E. (1927). Gravity on the earth and on the moon. *Sci. Mon. N.Y.* **24**, 448–462.

Wright, F. E. (in press). The surface of the Moon. In "The Solar System" (G. P. Kuiper, ed.), Vol. 4, Planets and Comets, Pt. II. Chicago Univ. Press, Chicago, Ill.